Analysis of the Differentiation of Adult Neural Stem and Progenitor Cells Post Treatment with the ASH1 Transcription Factor

A Thesis

Submitted to the Faculty of Graduate Studies and Research

In Partial Fulfillment of the Requirements

For the Degree of

Master of Science

In

Biology

University of Regina

By

Shaneen Michelle Teece

Regina, Saskatchewan

March, 2018

UNIVERSITY OF REGINA

FACULTY OF GRADUATE STUDIES AND RESEARCH

SUPERVISORY AND EXAMINING COMMITTEE

Shaneen Michelle Teece, candidate for the degree of Master of Science in Biology**,** has presented a thesis titled, ***Analysis of the Differentiation of Adult Neural Stem and Progenitor Cells Post Treatment With the ASH1 Transcription Factor,*** in an oral examination held on March 19, 2018. The following committee members have found the thesis acceptable in form and content, and that the candidate demonstrated satisfactory knowledge of the subject material.

External Examiner:	*Dr. Veronica Campanucci, University of Saskatchewan
Supervisor:	Dr. Josef Buttigieg, Department of Biology
Committee Member:	Dr. Melanie Hart, Department of BIology
Chair of Defense:	Dr. Nader Mobed, Department of Physics

*via video conference

Abstract

Adult neural stem and progenitor cells hold the potential to regenerate lost tissue following injury or disease to the central nervous system. Before these cells can be used to regenerate tissue, they must be instructed to differentiate into the appropriate cell type. The objectives of this thesis were to investigate the differentiation induced from the proneural transcription factor ASH1 with an intracellular delivery mechanism in adult neural stem and progenitor cells cultured *in vit*ro and to develop an in-house biosensor capable of detecting the neurotransmitter glutamate from non-myelinated axons. It was demonstrated that the addition of the cell permeable ASH1 promoted neurogenesis in neural stem and progenitor cells after two weeks of cell culture. Patch-clamp electrophysiology and immunocytochemistry were used to verify that the cells were differentiating into neurons. Although the cells did not develop into mature neurons capable of generating action potentials, they showed neuronal characteristics including the expression of neurofilament and the presence of voltage-gated Na+ channels. In addition, it was shown, using patch-clamp electrophysiology on HEK293T cells transduced to express the glutamate ionotropic receptor GRIK3, that glutamate can be detected in the bath solution. This work shows that HASH1 can be used to induce neuronal differentiation in adult neural stem and progenitor cells *in vitro* and the in-house biosensor can be used to detect potential glutamate release from axons of neurons generated by ASH1.

Acknowledgements

I would like to thank my supervisor, Dr. Josef Buttigieg for the opportunity, his mentorship and support in helping me achieve my MSc. I would also like to thank Anastasye Kisheev, Dr. Marianne Jacobsen and members of the Buttigieg lab for their guidance and support throughout this experience. Lastly, I would like to thank my committee member, Dr. Mel Hart, for her writing advice and help editing my thesis.

Dedication

For my husband, David Teece, who has provided me with the greatest love and support in helping me achieve my MSc.

Table of Contents

List of Figures

List of Abbreviations

AMPA	α-amino-3-hydroxy-5-methyl-4-isoxazolepropionic acid
Ara-C	Cytosine β-D-arabinofuranoside
ASH1	Achaete-scute homolog 1
ATP	Adenosine triphosphate
BK	bradykinin
Cm	Membrane capacitance
CNS	Central nervous system
DAPI	4',6-diamidino-2-phenylindol
DG	Dentate gyrus
DMEM	Dulbecco's Modified Eagle medium
DRG	Dorsal root ganglia
EGF	Epidermal growth factor
ERS	Extracellular recording solution
FBS	Fetal bovine serum
FGF	Fibroblast growth factor
GFAP	Glial fibrillary acidic protein
GFP	Green fluorescent protein
GFR	Growth factor reduced

GRIK3	Glutamate ionotropic receptor kainate type subunit 3
HASH1	Human achaete-scute homolog 1
iPSC	induced pluripotent stem cells
IRS	Intracellular recording solution
LTP	Long term potentiation
NF	Neurofilament
NMDA	N-methyl-D-aspartate
NSPC	Neural stem and progenitor cells
OB	Olfactory bulb
OL	Oligodendrocyte
OPC	Oligodendrocyte progenitor cells
PBS	Phosphate buffered solution
PDL	Poly-D-lysine
PS	Penicillin/streptomycin
SGZ	Subgranular zone
SVZ	Subventricular zone
TTX	Tetrodotoxin

Chapter 1. Introduction

1.1. Background

While stem cells are required for early neural development, pools of neural stem and progenitor cells (NSPC) remain active and continue to produce new cells within the adult central nervous system (CNS). The stem cells that remain through adulthood hold the potential to regenerate neurons or glial cells lost or damaged by neurodegenerative diseases such as multiple sclerosis or injury to the brain and spinal cord. Thus, it is not surprising that research in the field of regenerative therapy using stem cells has become increasingly popular. Despite many recent advances, there are numerous hurdles to overcome, such as the inability to stimulate endogenous stem cells post injury, or the requirements to induce differentiation of appropriate cell types from stem cells. The current understanding on how adult neural stem cells differentiate into the mature neural cell types still remains incomplete; therefore, *in vitro* experiments are valuable to give insight on how these processes may occur naturally within the brain.

1.2. Cells of the central nervous system

The CNS includes the brain and spinal cord and is made up of neurons and glial cells. Neurons process and transmit information by sending excitatory or inhibitory electrochemical signals to other neurons and cells. A typical neuron has a soma, many dendrites for receiving chemical signals, and a central axon to send electrochemical signals. The electrochemical signal consists of changes in membrane potential due to voltage-gated ion channels, known as the action potential, and the release of

neurotransmitters at the terminal button. The action potential triggers the release of neurotransmitters into the synapse, a small junction between the terminal of an axonal branch of the neuron sending the signal (pre-synaptic) and the receiving cell (post-synaptic). They then bind with receptors on the post-synaptic cell and generate excitatory or inhibitory responses.

Glial cells, oligodendrocytes, astrocytes and microglia are the most abundant cells in the CNS; they function to support many aspects of the nervous system. Oligodendrocytes (OL) are critical for proper neuronal function as they create the myelin sheath, a fatty insulation covering the axon (Morrison *et al.*, 2013). The myelin sheath speeds the action potential through saltatory conduction, a process whereby the action potential jumps between the unmyelinated nodes of Ranvier (Dupree *et al.*, 1999). OLs are also important for axonal integrity as the loss of OLs causes damage to the axon and can eventually lead to neuronal death (Morrison *et al.*, 2013). Astrocytes support neurons by performing various functions such as metabolic support, up-take of neurotransmitters and formation of glial scars after injury (Khakh & Sofroniew, 2015). Astrocytes have many functions because they are heterogeneous cells that vary in morphology and function depending on the region of the brain and the type of neuron they support (Khakh & Sofroniew, 2015). Microglia are the immune cells of the CNS and have similar characteristics as macrophages to help protect the CNS from infection (Ginhoux *et al.*, 2013). Unlike the other neural cell types that are derived from neural progenitors, most microglia are derived from primitive macrophages of the yolk sac in embryonic development (Ginhoux *et al.*, 2010).

1.3. Neural stem and progenitor cells

1.3.1. Neurogenic niches

Adult NSPCs are located in two major niches; the subventricular zone (SVZ) of the lateral ventricles (Lois & Alvarez-Buylla, 1993) and the subgranular zone (SGZ) in the dentate gyrus (DG) of the hippocampus (Altman & Das, 1965; Kaplan & Bell, 1984). Adult NSPCs are capable of differentiating into all three types of cells in the CNS: neurons, oligodendrocytes, and astrocytes. Three main cell types reside in the SVZ: type B, C, and A cells. Type B cells make contact with the ventricle and show astrocyte-like characteristics, as they are positive for the astrocyte marker glial fibrillary acid protein (GFAP) (Doetsch *et al.*, 1997). They divide slowly and produce type C cells known as transient amplifying cells because they divide rapidly to produce neuroblasts or type A cells that will become neurons of the olfactory bulb (OB). Neuroblasts from the SVZ migrate to the OB (Lois *et al.*, 1996), at the same time undergoing morphological changes to become granule and periglomerular interneurons (Winner *et al.*, 2002; Pierre-Marie *et al.*, 2014).

Like NSPCs in the SVZ, different cell types are found within the SGZ. There are type B cells that are GFAP+ astrocytes that divide to produce type D cells that in turn become neurons of the hippocampus (Seri *et al.*, 2001; Doetsch, 2003). Mouse NSPCs from the SGZ differentiate into dentate granule cells within the hippocampus and take four weeks to become fully integrated mature neurons (van Praag *et al.*, 2002; Esposito *et al.*, 2005). The immature cells migrate radially from the SGZ into the granular cell layer of the hippocampus (Esposito *et al.*, 2005). Focus will be on SVZ NSPCs because they are the source of neural stem cells in this thesis.

1.3.2. Neurogenesis

Neurogenesis in the SVZ is influenced by many factors released by neighboring cells, cell-cell interactions, and cell-extracellular matrix interactions. Newborn OB neurons go through distinct developmental stages; the neurons develop functional GABA receptors prior to development of functional glutamate receptors and dendritic spines (Zhao *et al.*, 2008). They must then integrate with existing neuron circuitry and have the correct inputs to survive; half of the newborn neurons in the OB do not survive the first two months (Winner *et al.*, 2002).

Achaete-scute homolog 1 (ASH1) is a proneural transcription factor that belongs in the basic helix-loop-helix family of proteins encoded by the gene ascl1. ASH1 has a well-defined role in neurogenesis of the embryonic telencephalon; much of what we know about ASH-1 has been found in embryonic stem cells (Aiba *et al.*, 2006; Henke *et al.*, 2009; Castro *et al.*, 2011). ASH1 is also expressed in NSPCs in the SVZ (Ponti *et al.*, 2013) and the DG of the hippocampus in the adult mammalian brain (Kim *et al.*, 2007). There are many targets of ASH-1 including genes involved in proliferation, regulation of the cell cycle, promotion of neural differentiation and neurotransmitter biosynthesis including glutamate (Castro *et al.*, 2011). ASH1 produces both glutamatergic and GABAergic neurons in the adult brain (Kim *et al.*, 2007).

ASH1 also inhibits neurogenesis in neighboring cells by upregulating the expression of Notch signaling ligands such as Delta-like1 and Jagged1 (Imayoshi & Kageyama, 2014). Therefore, a role of the Notch signaling pathway is for the maintenance of NSPCs to ensure that the stem cell pool is not depleted when NSPCs

differentiate into neurons (Imayoshi *et al.*, 2010).The Notch signaling pathway is carried out by cell-cell interactions and the Notch ligands are surface proteins that interact with the Notch receptors on adjacent cells. Once the ligand binds with the Notch receptor it causes the release of the Notch intracellular domain from the transmembrane portion and goes to the nucleus to alter gene expression, thus promoting neurogenesis (D'Souza *et al.*, 2008). Activation of the Notch pathway in neighboring NSPCs induces the expression of transcriptional repressors such as hairy and enhancer of split that prevent the expression of proneural genes (Imayoshi *et al.*, 2010). Furthermore, it has been reported that ASH1 can promote oligodendrogenesis and myelination in the postnatal brain (Nakatani *et al.*, 2013).

While there are many transcription factors involved with neural differentiation, it has been suggested that ASH1 is sufficient on its own to drive neuronal differentiation in induced pluripotent stem cells (iPSCs) (Chanda *et al.*, 2014). In other systems, addition of ASH1 was sufficient to induce glutamatergic neuron differentiation with rapid single step induction of iPSCs (Zhang *et al.*, 2013; Chanda *et al.*, 2014). A challenge with using a transcription factor to drive differentiation is how to deliver the factor to the cell, such as, cell viability, efficacy of transduction and insertion location of the plasmid. One means of delivery is by viral transduction; however, various problems can arise when inserting a gene into a cell. An alternative strategy for delivery is to modify the protein in such a way that allows the cell to uptake the protein and translocate it to the nucleus (Robinson *et al.*, 2016). iProgen Biotech has developed a novel protein delivery mechanism that enables protein uptake by cells by creating recombinant fusion proteins. This novel mechanism fuses the protein of interest with a secretion signal peptide

sequence followed by a cleavage inhibition signal (Lee et al., 2014). This delivery mechanism has been tested in human iPSCs; addition to the cell culture caused mature neurons to develop with a high number of branch points (Robinson *et al.*, 2016), but this delivery system has not been tested with adult NSPCs and this is one of the objectives of this project.

1.3.3. Oligodendrogenesis

Most subventricular zone NSPCs become neurons in the OB, but they can also differentiate into oligodendrocyte precursor cells (OPCs) and into mature OLs. There are four stages in OL development: OPC, preoligodendrocytes, immature (pre-myelinating) OLs and mature (myelinating) OLs (Barateiro & Fernandes, 2014). OPCs are proliferative and migratory cells whereas mature OLs are not and produce myelin (Bercury & Macklin, 2015). There are many intrinsic and extrinsic factors such as extracellular matrix molecules, and the release of neurotransmitters that regulate gene expression that direct OPCs through the OL lineage (Bercury & Macklin, 2015).

1.3.4. Culturing NSPCs in vitro

When NSPCs are cultured *in vitro* in the presence of the mitogens epidermal growth factor (EGF) and fibroblast growth factor (FGF) they grow as free floating cell aggregates known as neurospheres (Reynolds & Weiss, 1992). The neurosphere is a heterogeneous population of multipotent stem cells, neural precursors and glial precursors that can vary in cell function and life cycle such as mitosis, apoptosis and phagocytosis based on the location within the sphere (Bez *et al.*, 2003). Mitogens regulate the cell cycle as withdrawal of EGF or FGF promotes the differentiation of

NSPCs into neurons and glial cells (Johe *et al.*, 1996). The majority of the cells isolated from the SVZ are transient amplifying cells (C cells), which are responsive to EGF and are responsible for neurosphere formation (Doetsch *et al.*, 2002). When the NSPCs are grown in the presence of EGF *in vitro*, the amplifying cells (C cells) diverge from their path toward OB neurons and become multipotent, self-renewing progenitor cells capable of becoming neurons and glial cells (Doetsch *et al.*, 2002). Addition of other driving factors is often required to differentiate NSPCs more efficiently into desired brain cell types *in vitro.*

1.4. Glutamate receptors

Glutamate is the most abundant excitatory amino acid neurotransmitter in the nervous system (Curtis *et al.*, 1960). In addition to excitatory transmission, activation of glutamate receptors regulates many physiological aspects of the CNS including learning, memory and regeneration. Neurons and glial cells respond to glutamate via metabotropic and ionotropic receptors. Metabotropic glutamate receptors are G-protein coupled receptors that initiate various signaling cascades and increases intracellular calcium (Willard & Koochekpour, 2013). In contrast, the ionotropic glutamate receptors allow the flow of cations into the cell and increase membrane potentials (Rosenmund *et al.*, 1997). There are three recognized ionotropic subtypes that are named for the artificial agonists that interact with the receptors: α-amino-3-hydroxy-5-methyl-4-isoxazolepropionic acid (AMPA), N-methyl-D-aspartate (NMDA), and kainate receptors. Excessive stimulation of glutamate receptors can result in excitotoxicity whereby there is an increase in calcium ions within the neuron that leads to apoptosis and is implicated in many neurodegenerative diseases and injuries (Dong *et al.*, 2009).

AMPA and kainate receptors are permeable to Na^+ and K^+ upon activation by glutamate and their receptor agonists (Sobolevsky *et al.*, 2009; Traynelis *et al.*, 2010). AMPA receptors are the primary mediators of excitatory transmission by glutamate as they are the most abundant ionotropic glutamate receptor in the postsynaptic membrane and play a role in synaptic plasticity (Traynelis *et al.*, 2010). Kainate receptors are found on both presynaptic and postsynaptic membranes (Lerma, 2003). Kainate receptors on postsynaptic membranes contribute to synaptic transmission, but do not produce as much current as, and desensitize slower than, AMPA receptors (Castillo *et al.*, 1997). In the hippocampus, kainate receptors on the presynaptic membrane regulate glutamate release (Chittajallu *et al.*, 1996).

NMDA receptors are unique compared to the other ionotropic glutamate receptors because they allow the entry of calcium ions in addition to sodium and potassium ions (Traynelis *et al.*, 2010). NMDA receptors also require glycine for activation (Kleckner & Dingledine, 1988). Furthermore, there is a magnesium ion blocking the channel at resting membrane potential; depolarization of the membrane removes the magnesium ion from the channel. For ion movement through the NMDA receptor there needs to be a strong depolarization; and, at higher frequencies, because of these unique features, the NMDA receptor has a role in synaptic plasticity through long-term potentiation (LTP) (Lüscher & Malenka, 2012). NMDA facilitate LTP by triggering intracellular signaling cascades from the influx of calcium that increase the density of AMPA receptors in the postsynaptic membrane, thereby strengthening synaptic transmission (Matsuzaki *et al.*, 2004).

1.5. Myelination

In healthy adults new OLs and myelin are generated continuously throughout life and have been suggested as a form of plasticity important in learning in the brain (Young *et al.*, 2013; Yeung *et al.*, 2014). For myelination to occur, communication between migrating OPCs and unmyelinated axons is required to help guide OPCS to the unmyelinated axons. While it is not clear what endogenous cues help guide OPCs to axons, evidence suggests secreted factors such as the neurotransmitters glutamate and adenosine triphosphate (ATP) may play a role. Several studies have shown that glutamate promotes OL differentiation and the production of myelin (Cavaliere *et al.*, 2012; Li *et al.*, 2013). OPCs express glutamate ionotropic and metabotropic receptors, suggesting that glutamate is likely a key regulator of OPCs and myelination. It has been reported that electrical activity from non-myelinated neurons and activation of the AMPA receptors promotes OPCs to become myelinating OLs (Fannon *et al.*, 2015; Gautier *et al.*, 2015). However, there are inconsistencies in the literature because the NMDA receptor has also been reported to have a role in the regulation of OPCs (Cavaliere *et al.*, 2012; Li *et al.*, 2013; Gautier *et al.*, 2015).

While ATP is known as a form of energy storage in the cell, it has also been shown to be a neurotransmitter, playing a role in myelination, and can interact with OPCs and astrocytes (Stevens *et al.*, 2002; Ishibashi *et al.*, 2006). ATP is rapidly hydrolyzed to adenosine, with both capable of binding to purinergic receptors. It has been demonstrated that OPCs express purinergic receptors and activation by adenosine promotes OPC differentiation and myelination (Stevens *et al.*, 2002). In addition, glial - glial interactions have a role in the myelination process; cross-talk between astrocytes

and OLs has been suggested to increase myelination (Ishibashi *et al.*, 2006). It has been demonstrated that ATP released from non-myelinated axons can activate purinergic receptors on nearby astrocytes causing the release of leukemia inhibitory factor and promoting OPC differentiation (Ishibashi *et al.*, 2006).

1.6. DRG neurons

Doral root ganglia (DRG) neurons are clusters of sensory neurons located alongside the spinal cord, and release glutamate *in vivo* and *in vitro* (Rydh-Rinder *et al.*, 2001; Krames, 2014). DRGs are peripheral nervous system neurons that extend axons into the CNS to relay sensory information (Krames, 2014). DRG neurons are often used in *in vitro* myelination experiments because they are easy to isolate, grow new axons in cell culture, and can be myelinated by OLs in co-culture systems (Shaw & Compston, 1996; Liu *et al.*, 2013).

1.7. Patch-clamp electrophysiology

Patch-clamp electrophysiology is a technique that allows the study of whole cell ion channels or single ion channels in biological membranes (Penner, 2009), and thus gives insight to cellular interpretation of environmental stimuli. This technique was first used by Erwin Neher and Bert Sakmann to describe single channel currents of acetylcholine receptors in frog muscle fibers (Neher & Sakmann, 1976). Since then patch-clamp electrophysiology has been used to study many different types of biological membranes and ion channels. The patch clamp technique involves placing a glass micropipette with a recording electrode containing ionic solution onto a biological membrane. Negative suction is applied, creating a tight seal with high electrical

resistance around the membrane. The membrane within the pipette is referred to as a patch (Neher & Sakmann, 1976). This technique was developed to reduce electrical noise and enable researchers to study single channel currents (Neher, 1992). (Neher, 1992). However, it was not until 1980 with the development of the "Gigaseal" that the background noise was reduced considerably and gave higher resolution recordings (Neher, 1992). A gigaseal is created when negative suction is applied to the patch pipette in the on-cell configuration; a patch of membrane is sucked into the interior of the pipette and prevents the leakage of ions between the pipette and the bath solution (Sakmann & Neher, 1984). The gigaseal allowed for the development of the many patch-clamp configurations.

The most basic patch clamp configuration, and the starting point of all other configurations, is the on-cell. To obtain the on-cell configuration the patch pipette is placed onto a cell and suction is applied to get a gigaseal. With the on-cell, single channel currents within the patch can be measured. If the patch pipette is then withdrawn from the cell, a piece of membrane can be excised from the cell to give the inside-out configuration (Sakmann & Neher, 1984). It is called the inside-out because the inside of the cell membrane is facing the outside environment. The whole cell configuration is obtained by rupturing the cell membrane within the patch. This establishes an electrical connection between the cell's interior and the pipette and allows for whole cell currents to be recorded (Sakmann & Neher, 1984). The outside-out configuration is obtained when the pipette is withdrawn from the whole cell configuration to create an excised piece of membrane with the outside portion of the membrane facing the outside environment of the bath solution (Sakmann & Neher, 1984).

The whole cell configuration is useful to study whole cell currents; however, because the interior of the cell is continuous with the pipette, the cytosol gets washed out and cell function is lost. To prevent cytosol and functionality loss, perforated patch was developed. The perforated patch uses antibiotics that create small pores in the cell membrane which only allows the passage of monovalent ions, and prevents the cell's interior from washing out (Akaike & Harata, 1994). The antibiotics nystatin and amphotericin B are polyene antibiotics produced by the bacteria *Streptomyces nodosus,* and are commonly used to create the perforated patch (Akaike & Harata, 1994).

A different configuration of patch-clamp electrophysiology is the sniffer patch that combines the outside-out configuration to create a biosensor for the release of compounds such as neurotransmitters. The sniffer-patch was first used to detect the release of acetylcholine from growth cones of developing neurons (Hume et al., 1983, Young & Poo, 1983), and has been used to detect the release of other neurotransmitters including ATP (Silinsky & Redman, 1996), glutamate (Copenhagen & Jahr, 1989), and GABA (Christensen *et al.*, 2014). In the outside-out configuration, a patch of membrane is excised from a donor cell with an ionotropic neurotransmitter receptor to detect neurotransmitter release.

1.8. Hypotheses and objectives

1.8.1. Hypothesis 1

Traditionally, neurons are described as only releasing neurotransmitters from the synapse; however, several lines of evidence suggest that neurotransmitters are also released along axons. Since it has been shown that OPCs require glutamate to

differentiate and myelinate neurons, it is hypothesized that non-myelinated axons release neurotransmitters directly from axons providing a cue for migrating OPCs.

1.8.2. Objective 1

The objective is to detect the release of glutamate from non-myelinated DRG neurons using the sniffer patch technique. HEK293T cells that express the glutamate ionotropic receptor kainate type subunit 3 (GRIK3) will be used to verify glutamate detection and development of the sniffer patch to detect possible locations of glutamate release on non-myelinated axons.

1.8.3. Hypothesis 2

ASH-1 is a proneural factor required for neurogenesis. iProgen Biotech has developed a cell permeable human ASH1 (HASH1) peptide for delivery to the cell nucleus. This novel delivery mechanism has been tested in human iPSCs but has not been tested in adult NSPCs. Addition of the HASH1 peptide to adult NSPCs will induce neurogenesis.

1.8.4. Objective 2

The objectives in this collaboration with iProgen are to determine if the addition of the ASH-1 to cell culture can induce neural differentiation in NSPCs isolated from adult mice and also determine whether the differentiated neurons are glutamatergic (see objective 1). The withdrawal of EGF has shown that mitogen withdrawal can promote differentiation of NSPCs *in vitro*. Therefore, mitogen withdrawal will be used in combination with the cell permeable HASH1 peptide to determine the best conditions to

induce neurogenesis from NSPCs. Patch-clamp electrophysiology and immunocytochemistry will be used to determine if HASH1 can induce NSPCs develop into neurons *in vitro.*

Chapter 2. Materials and Methods

2.1. HEK293T cell culture

A previous student developed HEK293T cells expressing the GRIK3 receptor by lentivirus transduction to be used as a glutamate specific biosensor. HEK293T cells were cultured at 37 ºC and 5% CO_2 in Dulbecco's Modified Eagle Medium (DMEM) (Gibco, Cat. no. 11995) supplemented with 5% fetal bovine serum (FBS) (Gibco, Cat. No. 12483) and 1% penicillin/streptomycin (PS) (Gibco, Cat No. 15140). The cells were passaged every 7 days. The cells were detached from the dish with warmed (37 ºC) trypsin-EDTA (Gibco, Cat. No. 25200), which was left in the dish for 3 minutes. They were then collected and added to an equal portion of cell media to stop the trypsin digestion. The cells were centrifuged at 200 rcf for 2 minutes and the supernatant was removed before re-suspending the cells in HEK293T media. HEK293T cells were always plated with 500 000 cells in a 10cm cell culture dish. The cells were counted using a haemocytometer and trypan blue. HEK293T cells used for electrophysiology were plated on 25 mm coverslips coated with poly-D-lysine (PDL) (Corning, Cat. No. 354210). PDL was incubated on coverslips for 10 minutes, then washed with sterile type 1 water and allowed to dry for one hour prior to adding cells. The HEK293T cells were stored for 2 years in liquid nitrogen prior to use. The cells were thawed by warming to 37 ºC and adding 10ml of HEK293T media before placing in a 10 cm cell culture dish. The cells were allowed to attach over-night and the media was changed the following day.

2.2. DRG neuron isolation and cell culture

Dorsal root ganglia (DRG) neurons were isolated from adult mice euthanized by cervical dislocation. The spinal cord and surrounding tissue was removed and placed under a dissecting scope. The DRG neurons were removed from the thoracic and lumbar regions of the spinal cord and placed in sterile 1X phosphate buffered solution (PBS) with 4% PS. PBS was removed and placed in 5 mg/mL collagenase (Life Technologies, Cat. No. 17104). The DRGs were incubated at 37 ºC for 30 minutes and mechanically dissociated with a fire polished Pasteur pipette. The tissue suspension was centrifuged at 100 rcf for 30 seconds and the supernatant was collected. The supernatant was centrifuged to collect a pellet and removed. The pellet was re-suspended in DRG media with DMEM, Hams F12 (Gibco, Cat No. 11765), 1 % PS, 0.5 mM HEPES (Sigma, Cat No. H4034), 1X B27 neural supplement (Gibco, Cat. No. 12587), and 5% FBS. Fresh collagenase was added to the DRGs and incubated for another 30 minutes at 37 ºC. The tissue was mechanically dissociated with a fire polished Pasteur pipette of a smaller diameter than the one used in the first mechanical dissociation. DRG media was added to the tissue and incubated at 4 ºC for 10 minutes to allow the tissue debris to settle to the bottom. The supernatant containing the cells was collected and added to the cell suspension set aside previously. The cells were centrifuged at 200 rcf for 2 minutes and the supernatant was removed. The pellet containing the DRG neurons was suspended in DRG media and set aside in the incubator The DRG neurons were cultured on 25 mm coverslips coated with growth factor reduced (GFR) Matrigel (BD Biosciences, Cat. No. 354230). Matrigel was added to coverslips and incubated at room temperature for 30 minutes. The matrigel was removed and the coverslips were washed twice with sterile

type 1 water and allowed to dry. Each coverslip was plated with 500 µL of suspended DRGs and allowed to attach overnight. The culture dish was flooded with DRG media supplemented with 5 µM cytosine β-D-arabinofuranoside (ara-C) (Sigma, Cat. No. C1768) for one day to kill any mitotic cells. Fresh DRG media was added the following day to remove ara-C from the cell culture. The DRG neurons were cultured at 37 ºC and 5% CO_2 for minimum one week prior to electrophysiology experiments.

2.3. NSPC isolation and cell culture

NSPCs were isolated from the subventricular zone (SVZ) of adult mice euthanized by cervical dislocation. The brain was removed and placed under a dissection microscope to remove the tissue surrounding the SVZ and the olfactory bulb. The tissue was placed in sterile 1X PBS and 4% PS. The PBS was removed, replaced with 5 mg/mL collagenase, and incubated at 37 ºC with trituration every 30 minutes. The digested tissues was suspended in NSPC stock media with DMEM, Hams F12, 1% PS, and 0.5 mM HEPES and incubated at 4 ºC for 10 minutes. The supernatant was collected and centrifuged at 200 rcf for 2 minutes. The supernatant was removed and the pellet was suspended in NSPC working media with NSPCs stock media, 1X B27 supplement, 20 ng/mL human basic fibroblast growth factor-2 (bFGF) (Gibco, Cat. No. PHG0024), 20 ng/mL EGF (Gibco, Cat. No. PHG0313), and 10 µg/mL heparin (Sigma, Cat. No. 1001352521). NSPCs were cultured in T25 culture flasks in NSPC working media and passaged every 5-6 days. NSPCs were passaged by collecting cells and centrifuged at 200 rcf for 2 minutes. The supernatant was removed and the pellet was re-suspended in 1 mL of the dissociation reagent TryplE (Gibco, Cat. No. 12605028) and incubated at 37 ºC for 20 minutes with trituration at 10 minutes to ensure proper neurosphere

dissociation. The cells were diluted with 1 mL NSPC stock media and triturated 50X with a Pasteur pipette to break up neurospheres. The cells were centrifuged and the supernatant was removed. The cell pellet was re-suspended in NSPC working media and plated at 100 000 cells/mL. The cells were counted with a hemocytometer and trypan blue. NSPC stocks were kept in liquid nitrogen. The NSPCs were stored with $2x10^6$ cells/cryogenic vial in 10% DMSO and NSPC stock media. The temperature was reduced slowly, first placing the cells for one hour each at 4 ºC, -20 ºC, and -80 ºC prior to the liquid nitrogen for long-term storage (up to 2 years). The NSPCs were thawed by warming the cryogenic vial to 37 ºC and diluting with 10 mL NSPC stock media, then to a GFR Matrigel coated 10 cm culture dish left overnight. The following day, the NSPCs were detached from the plate with 3 mL of TryplE for 3 minutes at 37 ºC. The cells were centrifuged at 200 rcf for 2 minutes then suspended in NSPCs working media and placed in a T25 culture flask. NSPCs used for electrophysiological recordings and immunocytochemistry were cultured on 25 mm coverslips coated with GFR Matrigel with approximately 2000 cells/coverslip in 500 µL and allowed to attach overnight. The culture dish was flooded with NSPC media the following day.

2.4. Electrophysiology set up

Extracellular recording solution (ERS) bathed the cells during electrophysiological recordings. The ERS contained the following in mM: 135 NaCl, 5 KCl, 2 $CaCl_2$, 2 $MgCl_2$ 10 glucose, and 10 HEPES in type I water; the pH was brought to 7.4 with NaOH before filtering the solution. To stimulate glutamatergic receptors, 10 mM glutamate was added to the ERS prior to adjusting pH. The whole cell recording solution used for the whole cell and the outside-out configurations contained the

following in mM: 110 K-gluconate, 25 KCl, 5 NaCl, 10 HEPES, 11 EGTA, and 2 MG-ATP in type I water and the pH was brought to 7.4 before with NaOH prior to filtering the solution. The internal recording solution used in the pipette contained the following in mM: 135 KCl, 5 NaCl, 2 $CaCl_2$ and 10 HEPES, and the pH was brought to 7.2 prior to filtering the solution. For perforated patch experiments 250 - 500 µg/mL of nystatin (Alta Aesar, Cat. No. J62486) in IRS was used. The inhibitors tetrodotoxin (TTX, 200nM) for voltage-gated Na^+ channels and cadmium chloride (CdCl, 50 µM) for voltage-gated Ca^{2+} were tested on NSPCs to determine presence of ion channels. The cell was first recorded in ERS, then with the inhibitor and lastly after the inhibitor was washed off with ERS.

Pipettes were made from borosilicate glass capillaries and were pulled with a Narishige PC-10 vertical pipette puller. Pipettes used for experiments had resistances in the 4 MΩ and 8 MΩ range. The recording electrodes were made of bleached silver wire (AgCl). An Axon instrument's CV 203B4 head stage was used and controlled with a Scientifica Patchstar micromanipulator. An Axopatch 200B amplifier was used with an Axon Digidata 1550 digitizer (Molecular Devices). On the amplifier, the output gain was set to 1X, lowpass filter was set to 5 kHz and the leak subtraction set to infinity. The bath mode was used to find the cell to obtain a gigaohm seal. The cell mode was used to record values for the cell. Experiments were done and analyzed with pClamp 10 software (Molecular Devices).

2.5. Immunocytochemistry

2.5.1. Immunocytochemistry for neurofilament

Immunocytochemistry was done to determine if NSPCs were expressing the heavy chain neurofilament (NF). To allow for optimal imaging, cells were grown on glass coverslips. The glass coverslips were removed from the dish and washed for 10 minutes three times with ice cold PBS and fixed with 4% paraformaldehyde (PFA) for 20 minutes. The PFA was washed off with ice cold PBS for 10 minutes three times. The cells were blocked for 30 minutes to one hour in a blocking solution containing 0.01% Triton X, 0.3 M glycine, 1X PBS, and 1% BSA. The blocking solution was removed and the primary antibody for the heavy chain NF in blocking solution was added (NF 1:500 Abcam, Ab8135) and incubated at room temperature for 2 hours. The primary antibody was washed off with ice cold PBS for 10 minutes three times. The secondary antibody in blocking solution (Alexa Fluor 488 1:1000, Abcam, Ab150061) was added and incubated for one hour at room temperature. The secondary antibody was washed off with ice cold PBS for 10 minutes three times. A negative control without the addition of the primary antibody was included to ensure specificity of the secondary antibody to the primary antibody. The nuclear stain DAPI was added to a microscope slide and the coverslip was placed onto the microscope slide. The DAPI was left over night to dry and the coverslip sealed with nail varnish. Stained cells were viewed on a Zeiss Axio Vert.A1 epifluorescence inverted microscope (Carl Zeiss) and processed with the ZEN 2011 Blue edition software (Carl Zeiss).

2.5.2. Immunocytochemistry for GRIK3

The protocol is similar to above but with some changes to primary antibody incubation time. The GRIK3 primary antibody (1:500, Abcam, Ab 101882) was incubated overnight at 4 ºC. The secondary antibody (Alexa Fluor 647, Abcam, Ab150083) was incubated for 2 hours at room temperature.

2.6. Glutamate sniffer patch experiments

A previous student developed HEK293T cells expressing the GRIK3 receptor subunit to be used as a glutamate specific biosensor. To verify if the HEK293T cells expressing the GRIK3 receptor could respond to glutamate, they were cultured on glass coverslips and recorded in the whole cell and outside-out patch configurations. After the whole cell configuration was attained, an outside-out patch was created and tested for response to glutamate by adding the glutamate solution to the bath solution by a gravity fed system and recording in a current-clamp to confirm the presence of a glutamate receptor in the patch. The first stage of the outside-out patch is generating an on-cell patch and was identified when the membrane resistance increased to at least 1 Gohm. There was little inward and outward in this configuration. The patch was ruptured by negative pressure applied with a 10 mL syringe forming a whole cell configuration. The pipette was then pulled away from the cell; if the patch still retained the Gohm seal, it was considered a successful outside-out patch.

2.7. HASH1 driving experiments

To verify if the addition of the cell permeable HASH1 fusion peptide induced NSPCs to differentiate into neurons, NSPCs were grown for one week with or without

the HASH1 protein and the growth factor EGF. Patch-clamp electrophysiology was used to determine if the NSPCs had functional characteristics of a neuron. Three biological replicates of NSPCs isolated from different adult mice were used in the HASH1 driving experiments. The NSPCs were cultured for one and two weeks in the presence and absence of 20 µg/mL HASH1 fusion peptide (iProgen) and 20 ng/mL EGF to promote neural differentiation. There were four treatment groups tested: EGF (NSPC working media), - EGF (NSPC incomplete media), HASH1 + EGF, and HASH1 - EGF. Partial media changes were done every 3-4 days with fresh media. All experiments were performed on cells at passages 5 to 10. Perforated patch-clamp electrophysiology with a voltage-clamp was done on NPSCs to determine if NSPCs had the electrophysiological characteristics of a neuron. The cell currents when held at 0 mV, 20 mV, and 40 mV were analyzed because these membrane potentials are in the biological range to stimulate an action potential from the neuron. In addition, the cells were stained for the heavy chain NF to determine if the cells were developing neurites. The Na^+ channel inhibitor TTX and Ca^{2+} channel inhibitor CdCl were used on a few cells to determine the presence of ion channels.

2.8. Statistical analysis

Statistical analysis was done with Origin 9 software and R. The data was tested for normality with the Kolmogorov-Smirnov test. To determine statistical differences between groups, one-way Anova and the Bonferroni post hoc tests were used.

Chapter 3. Results

3.1. HEK293T +GRIK3 Electrophysiology

To ensure they did express the subunit, immunocytochemistry was performed to identify the GRIK3 subunit (Figure 1). Over 90% of the cells stained positive for the GRIK3 receptor subunit. These cells had similar morphology to control HEK293 cells. Furthermore, the plasmid construct used to generate the GRIK3 expressing cells had a GFP fusion peptide sequence; thus, the cells expressing the functional plasmid fluoresced green and made identification of the cells easier.

To validate the functionality of the GRIK3 receptor further, electrophysiology was performed on the cells. During a voltage-clamp, when a HEK293T cell was held at varying potentials, there was a dependent increase of current as membrane potential increased (Figure 2 A and B). In some experiments, glutamate was added to determine if the HEK293T cells expressing GRIK3 could respond to this neurotransmitter. In half of the whole-cell trials, the addition of glutamate did not elicit any significant change in whole cell membrane potential. In other trials following the addition of glutamate, there was an increase in membrane potential (Figure 2 C). The increase ranged from +10 mV to +50 mV. Washing the cells with recording solution returned the membrane potential to rest.

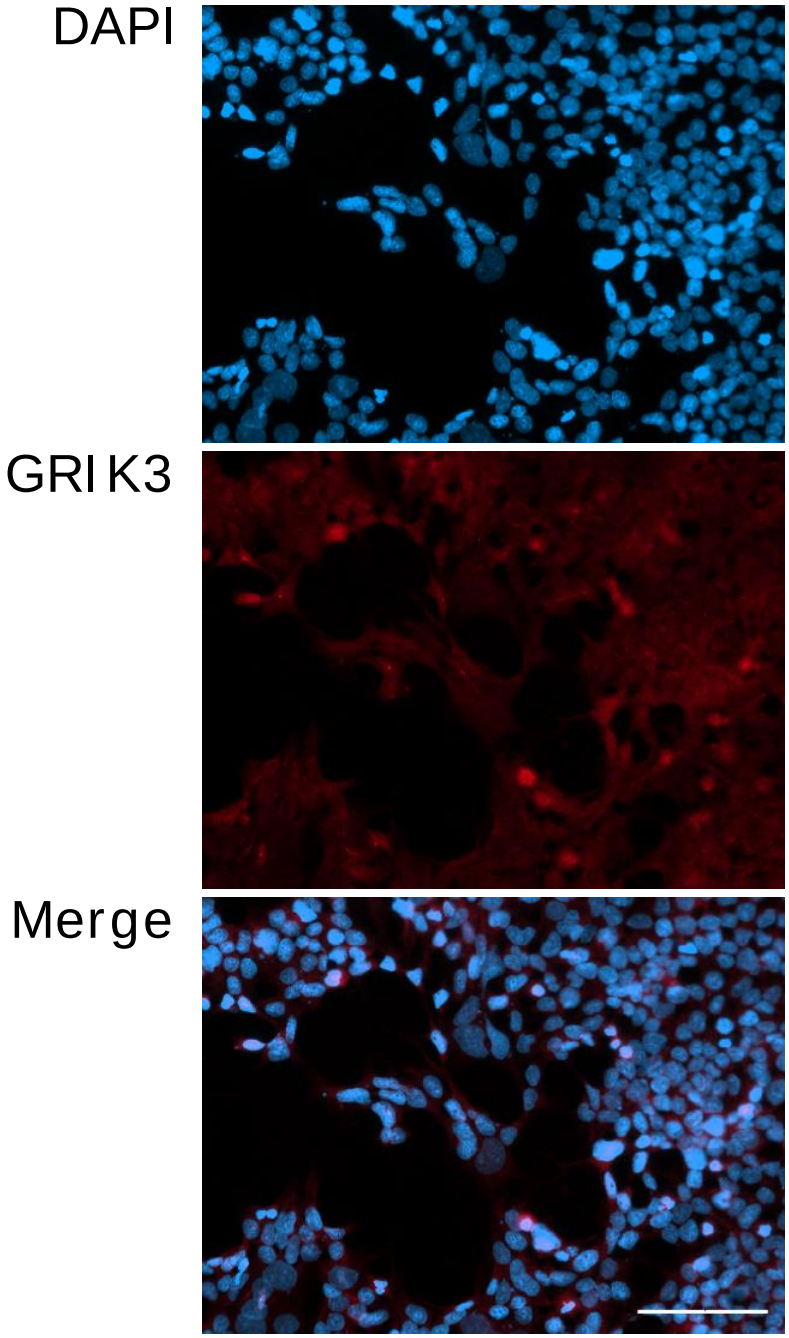

Figure 1. Immunocytochemistry for the GRIK3 subunit on HEK293T cells. Immunocytochemistry was done on HEK293T cells to detect the presence of the GRIK3 receptor subunit. Cells were stained for GRIK3 (red) and the nuclear stain DAPI (blue). Images were taken at 200X and the scale bar is 100 µm.

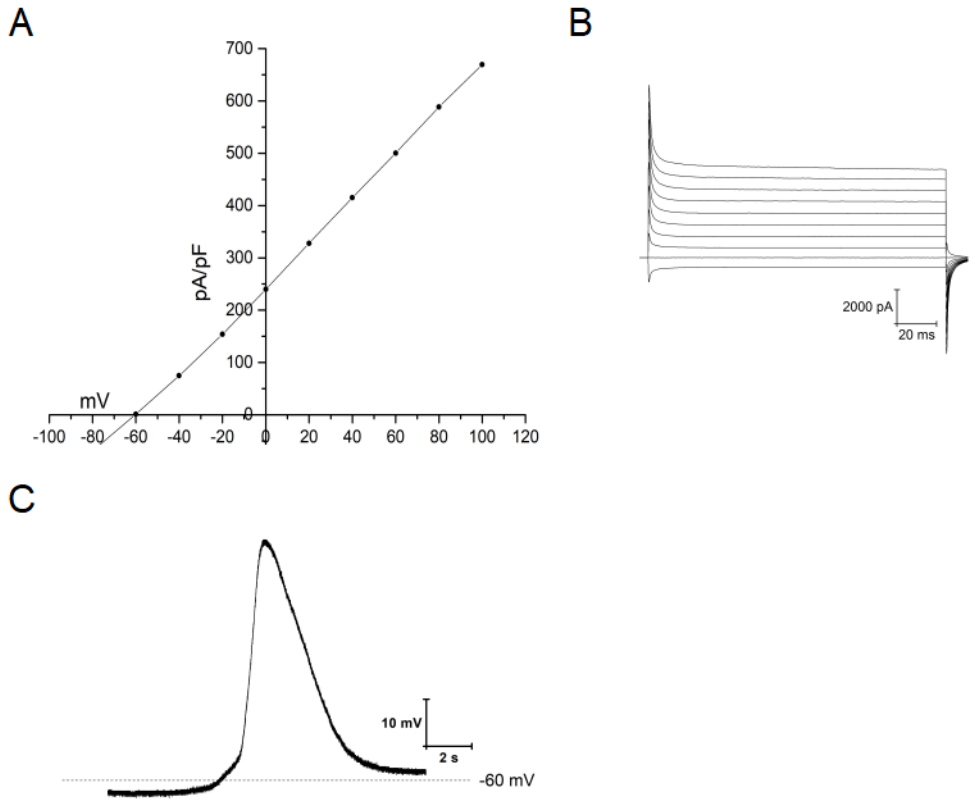

Figure 2.Patch-clamp electrophysiology on a HEK293T cell expressing the GRIK3 receptor in the whole cell configuration. The current (pA) versus voltage (mV) of a HEK293T cell expressing the GRIK3 receptor (A) and the current trace from the voltage-clamp (B) in the whole-cell configuration is shown. There was an increase in membrane potential following the addition of 10 mM glutamate (C).

The purpose of the biosensor was to develop an excised patch of membrane containing the GRIK3 receptor and be used to detect glutamate release. To demonstrate this capability, an outside-out patch was created from HEK293T cells (Figure 3). During current-clamp recordings, a baseline membrane potential of - 55 mV was observed; this was close to predicted values between the pipette and recording bath solutions. In some instances, there were no changes in membrane potential after addition of glutamate in the bath solution. In these cases, it was assumed that no ion channel or some other non-glutamate ion channel was present (Figure 4). In other preparations, glutamate caused a reversible increase of 5 mV to 10 mV in membrane potential (Figure 3C).

3.2. DRG neurons

Patch-clamp electrophysiology was done on DRG neurons to generate an electrical profile of a neuron to be used to identify derived neurons from driven NSPCs. When neurons were held at varying membrane potentials, there were large inward currents independent of membrane voltage as determined by significant variances in slope (Figure 5 A and B). During current-clamp recordings, it was observed that the resting membrane potential of a DRG neuron varied between - 40 mV to - 65 mV and there were small, spontaneous changes in membrane potential observed in some cells (Figure 5 C). To identify neuronal identity further, immunocytochemistry was done on DRG neurons to visualize neurofilament on a mature neuron to compare to NSPCs in driving experiments. DRG neurons stained positive for NF in the axon and dendrites which can be seen as long filaments (Figure 6).

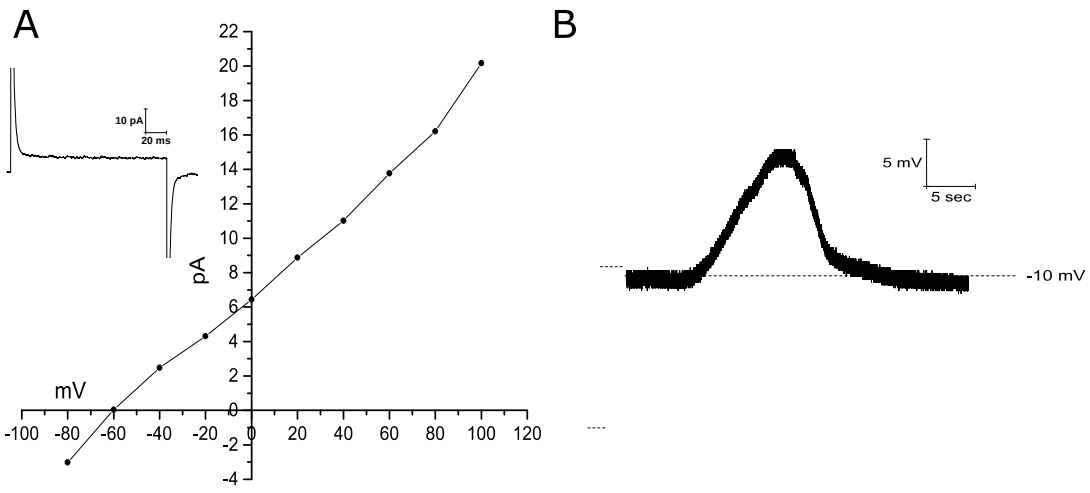

Figure 3. Outside-out patch with GRIK3 receptor from a HEK293T cell. The current-density (pA/pF) versus voltage (mV) plot in the outside-out configuration from a HEK293T cell with a representative trace at 0 mV inserted. There was an increase in membrane potential following the addition of 10 mM glutamate (B).

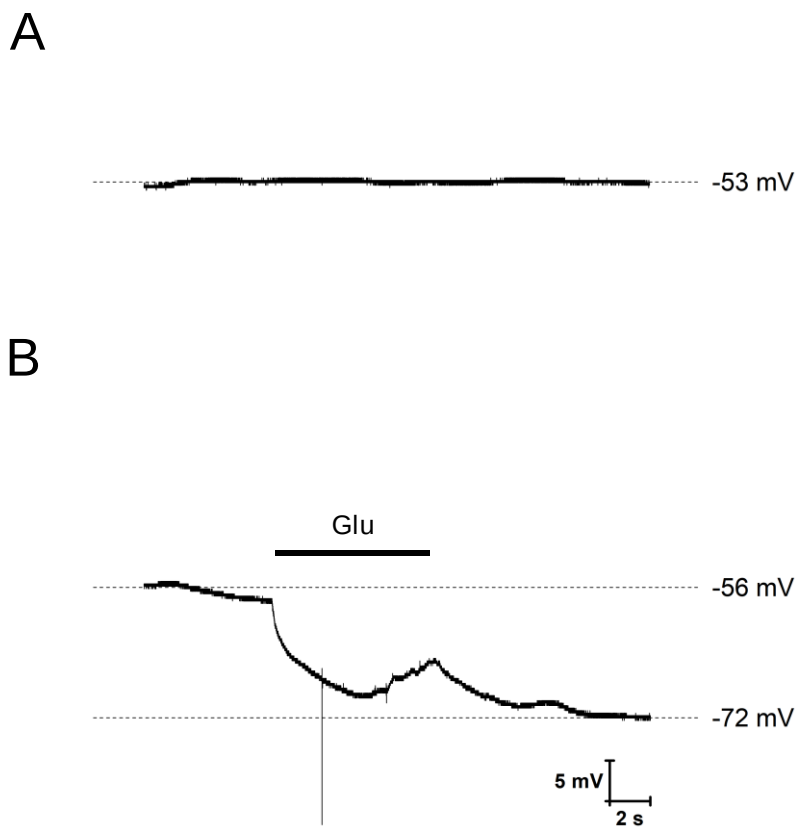

Figure 4. Whole-cell and outside-out patch membrane potentials of a HEK293T cell. The membrane potential (mV) of a HEK293T cell in whole-cell (A) and the membrane potential in the outside-out configuration (B) is shown. After the addition of glutamate to the outside-out patch, the membrane potential decreased; washing the cells did not return to initial membrane potential.

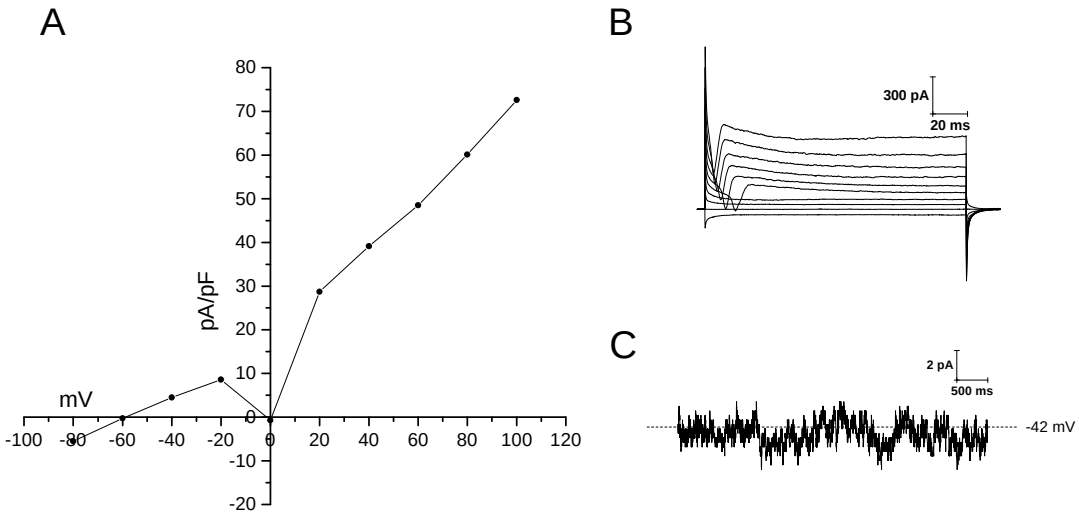

Figure 5. Patch-clamp electrophysiology of a DRG neuron grown in vitro. The current-density (pA/pF) versus voltage (mV) of a DRG neuron grown for 6 DIV at 30 ms (A), the current (pA) from the voltage-clamp recording (B), and the membrane potential (mV) of the neuron with small spontaneous changes in the membrane potential (C) is shown.

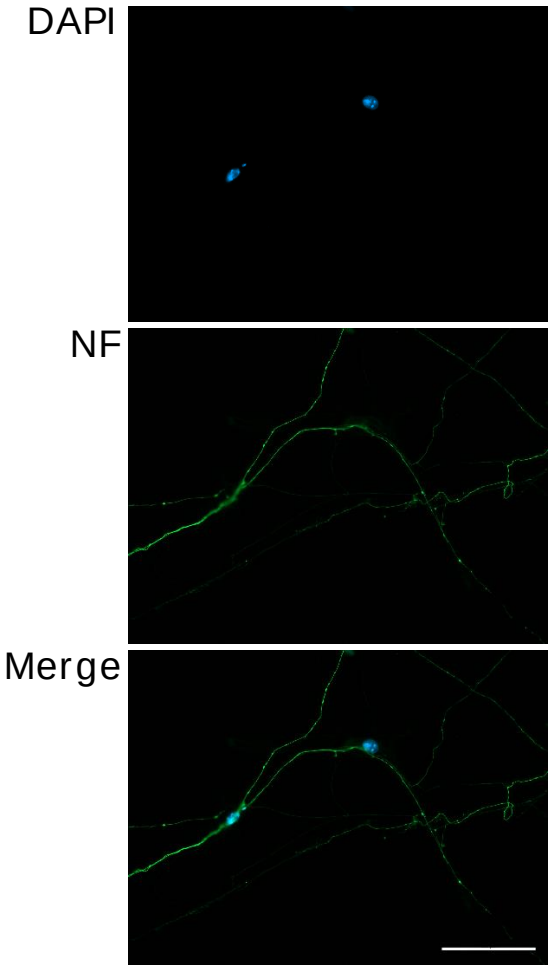

Figure 6. Immunocytochemistry for neurofilament on a DRG neuron.
Immunocytochemistry was done on a DRG neuron grown *in vitro* for the nuclear stain DAPI (blue) and NF (green). Image is at 200X and the scale bar is 100 µm.

3.3. One week HASH1 driving experiments

3.3.1. Electrophysiology

The first factor examined was the membrane capacitance (Cm) because it is proportional to cell size; a larger cell will have higher current. Because the Cm is proportional to cell size, it can be used to standardize the differences in current in cells of varying sizes and compare to the larger cell size of a mature DRG neuron. The mean (± SEM) Cms (pF) for NSPCs treated with EGF (11.74 ± 0.15), - EGF (11.08 ± 0.19), HASH1 + EGF (11.56 ± 0.27), and HASH1 - EGF (11.54 ± 0.14) were not statistically different from each other (Anova, n=9, p=0.1) (Figure 7).

The current-density (pA/pF) versus voltage (mV) plots of NSPCs treated for one week is shown in Figure 8. When held at varying membrane potentials, the HASH1 treated groups had 1.15-fold higher currents than the groups not treated with HASH1. There was an inward current observed immediately after the capacitive transient (Figure 8 A and B) in 6 NSPCs in the EGF group, 5 NSPCs in the no EGF group, 7 NSPCs in the HASH1 + EGF group, and 5 NSPCs in the HASH1 - EGF group when held at potentials greater than 20 mV. There was also an outward current following the inward current (Figure 8 C) 1 NSPC in the EGF group, 3 NSPCs in the HASH1 + EGF group, and 1 NSPC in the HASH1 - EGF group. The mean (± SEM) current-densities (pA/pF) of NSPCs held at 20 mV, 50 ms into the recording treated with EGF (6.00 ± 0.27), - EGF (5.94 ± 0.29),

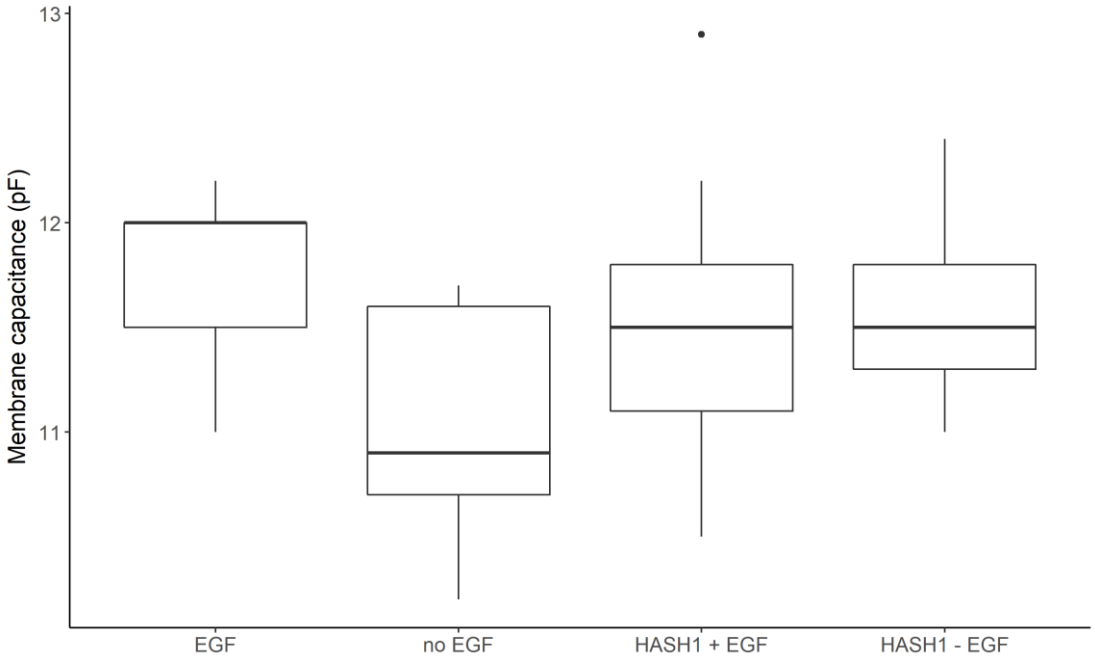

Figure 7. Membrane capacitances of NSPCs after one week of treatment. The membrane capacitances (pF) from cells grown with HASH1 ±EGF *in* vitro for one week are shown. The membrane capacitances were not statistically different between groups (Anova, n=9, p=0.1).

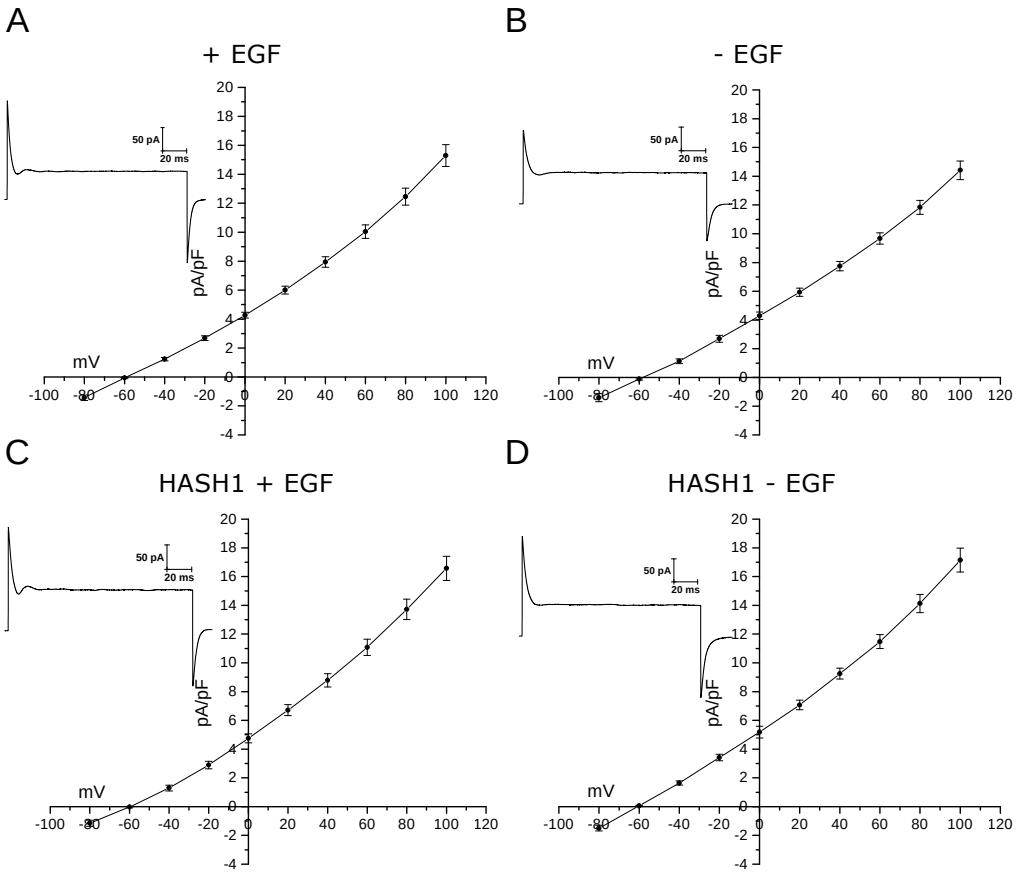

Figure 8. Patch-clamp electrophysiology of NSPCs after one week of treatment. The mean (± SEM) current-densities (pA/pF) versus voltage (mV) plots are shown for NSPCs grown in vitro for one week with EGF (A), without EGF (B), with HASH1 + EGF (C) and HASH1 - EGF (D). A representative electrophysiological current trace at 20 mV is inserted in each plot.

HASH1 + EGF (6.71 ± 0.39), and HASH1 - EGF (7.07 ± 0.33) were statistically different (Anova, p=0.013); however, the post hoc Bonferroni test showed no statistically significant pairwise comparisons (Figure 9). While not statistically different, the HASH1 protein elicited an increase in current-densities in both HASH1 treated groups when compared to the EGF and - EGF treated groups.

The total current amplitude was not steady over the duration of the recordings at the various potentials held. For example, while some groups had a transient decrease in outward current at various holding potentials, other groups had an increase in outward current over the duration of the recording. The transient inward current was observed between 13 ms and 43 ms, after the capacitive transient. To identify the characteristics of this current profile, the current anti-peak (min) amplitude, the mean, and peak (max) amplitudes (pA/pF) were taken for NSPCs held at 0 mV, 20 mV and the 40 mV in the time interval of 13 ms to 43 ms. Although all voltages are in the biological range, the focus was on 40 mV.

The anti-peak was considered for the inward current that followed the capacitive transient. The mean (± SEM) anti-peak amplitudes (pA/pF) of NSPCs treated with EGF (7.64 ± 0.37), no EGF (7.51 ± 0.47), HASH1 + EGF (8.27 ± 0.44), and HASH1 - EGF (9.03 ± 0.42) were not statistically different at 40 mV (Anova, p=0.06) (Figure 10). The same result was observed held at 0 V and 20 mV (Figures 11 and 12). The means (± SEM) of the mean amplitude (pA/pF) at 40 mV of NSPCs treated with EGF (8.14 ± 0.37), without EGF (7.89 ± 0.39), HASH1 + EGF (9.14 ± 0.43), and HASH1 - EGF (9.50 ± 0.38) were statistically different (Anova, p=0.017) at 40 mV (Figure 13). The post hoc test showed a statistically significant increase of current in the - EGF treated

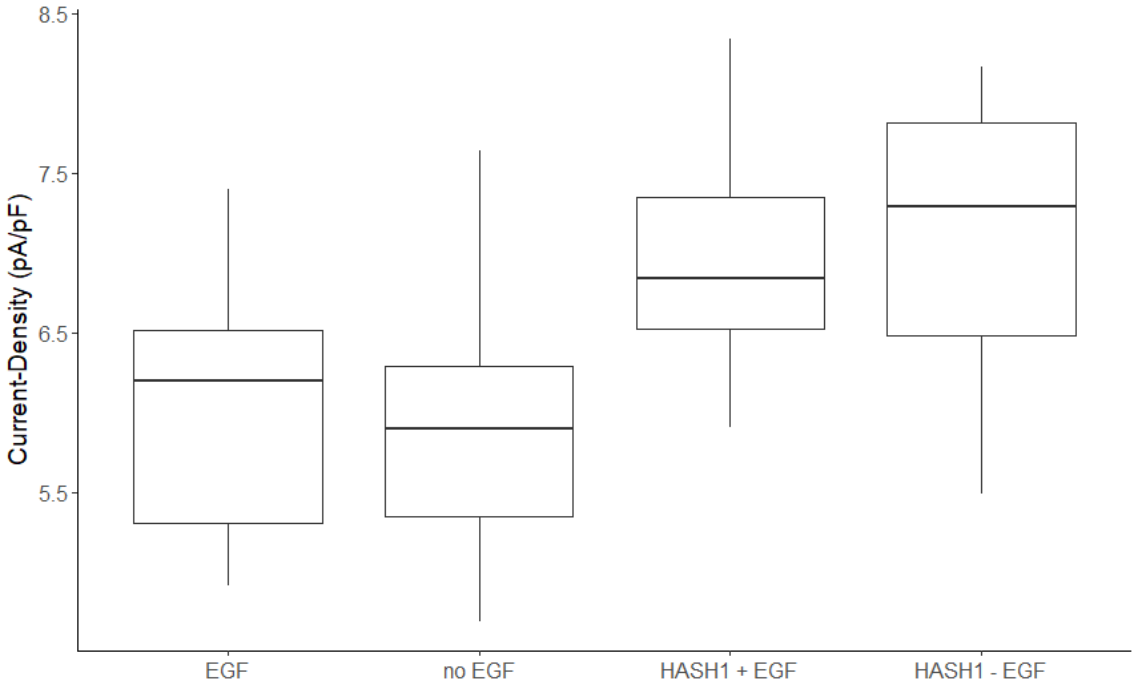

Figure 9. Current-densities of NSPCs treated for one week at 20 mV. The current-densities (pA/pF) at 50 ms into the electrophysiological recording of NSPCs treated with HASH1 ± EGF for one week *in vitro* are shown. The current-densities were statistically different (Anova, n=9, p=0.013); however, the Bonferroni post hoc did not demonstrate statistical differences between groups.

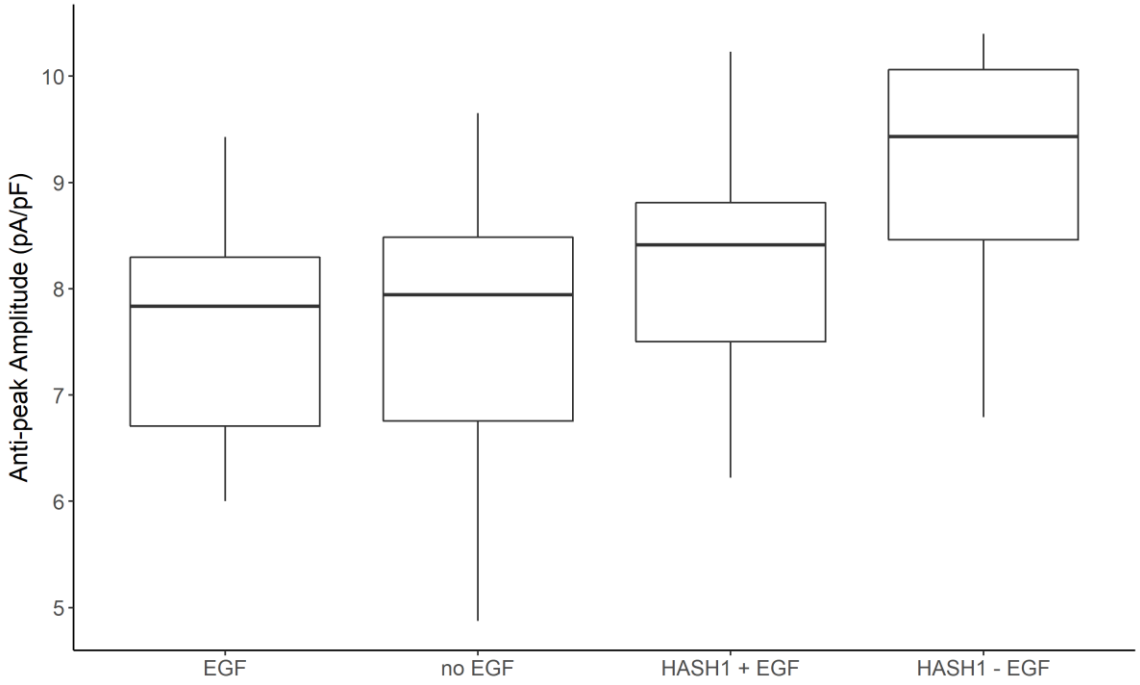

Figure 10. Anti-peak amplitudes of NSPCs after one week of treatment at 40 mV. The anti-peak amplitudes (pA/pF) of NSPCs grown with HASH1 ± EGF *in vitro* for one week between 13 ms and 43 ms of the electrophysiological recording are shown. The anti-peak currents were not statistically different between groups (Anova, n=9, p=0.06).

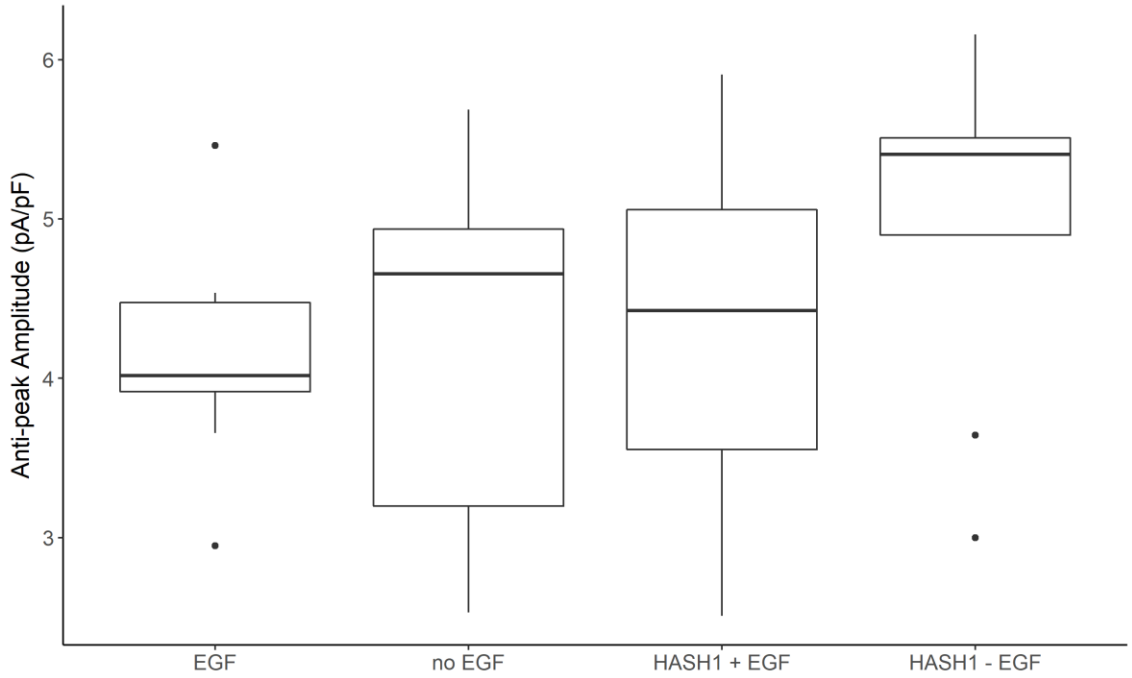

Figure 11. Anti-peak amplitudes of NSPCs after one week of treatment at 0 mV. The anti-peak amplitudes (pA/pF) of NSPCs treated with HASH1 ± EGF for one week *in vitro* between 13 ms and 43 ms of the electrophysiological recording are shown. The anti-peak currents were not statistically different between groups (Anova, n=9, p=0.25).

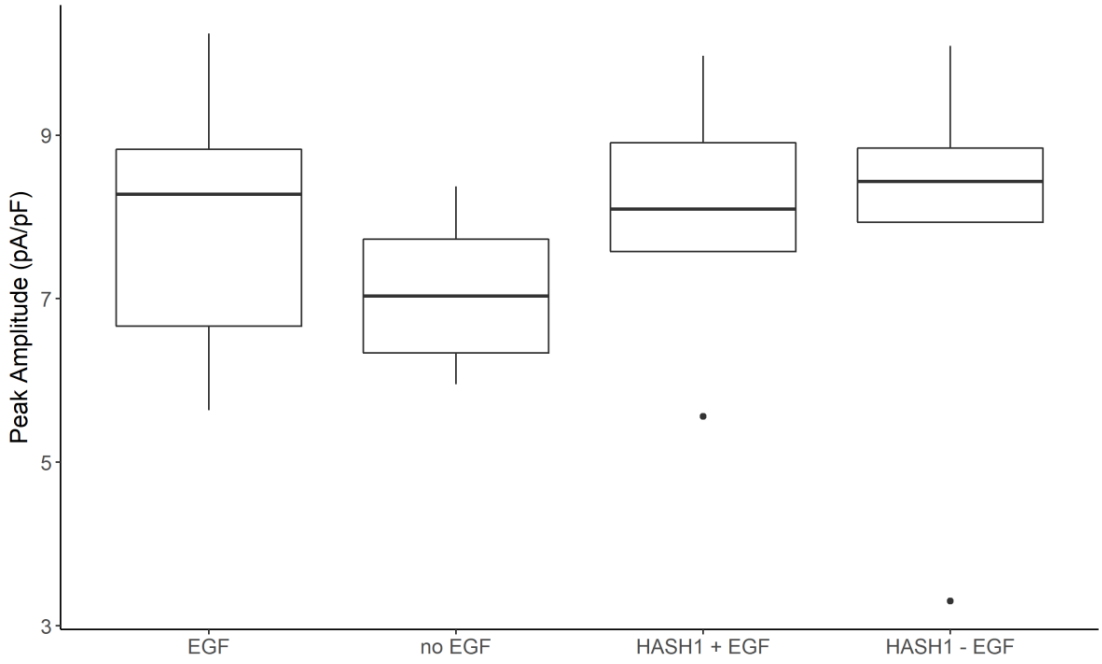

Figure 12. Anti-peak amplitude of NSPCs after one week of treatment at 20 mV. The anti-peak amplitudes (pA/pF) of NSPCs grown with HASH1 ± EGF *in vitro* for one week between 13 ms and 43 ms of the electrophysiological recording are shown. The anti-peak currents were not statistically different between groups (Anova, n=9, p=0.14).

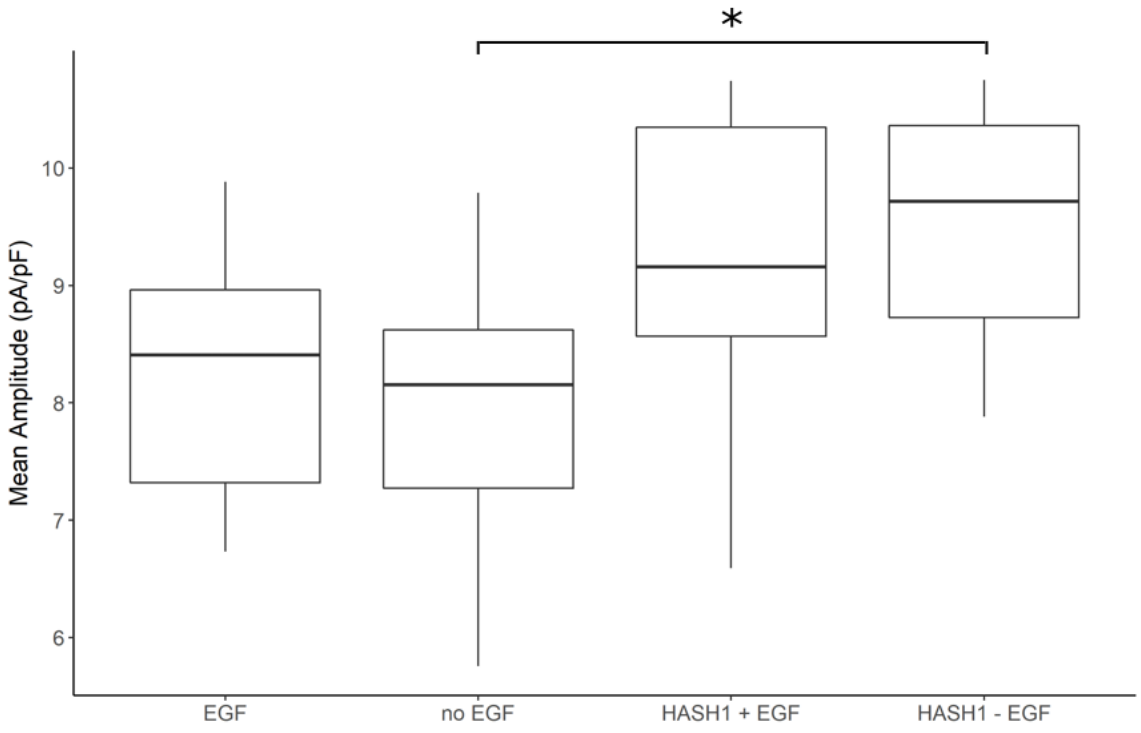

Figure 13. Mean amplitudes of NSPCs treated for one week at 40 mV. The mean amplitudes (pA/pF) of NSPCs grown with HASH1 ± EGF *in vitro* for one week between 13 ms to 43 ms of the electrophysiological recording are shown. The mean amplitudes were statistically different (Anova, n=9, p=0.017) and the post hoc showed that the - EGF and the HASH1 - EGF treated groups had different mean amplitudes (Bonferroni, p=0.039) and indicated by the asterisk.

group compared to the HASH1 - EGF treated group (Bonferroni, p=0.039). At 0 mV there were no statistical differences observed in the mean amplitudes (Anova, p=0.1) (Figure 14). In contrast, there was a statistical difference at 20 mV (Anova, p=0.04); however, the Bonferroni post hoc test demonstrated no differences between groups (Figure 15), the same result observed with the mean current-densities at 20 mV (Figure 9). In most recordings, the peak amplitude occurred at 13 ms during the decline of the capacitive transient; however, there was outward current following the inward current after the capacitive transient that occurred between 17 ms and 25 ms in the recordings of 1 NSPC in the EGF group, 3 NSPCs in the HASH1 + EGF group, and 1 NSPC in the HASH1 - EGF group. The mean (± SEM) peak amplitudes (pA/pF) of NSPCs treated with EGF (10.02 ± 0.62), - EGF (8.94 ± 0.37), HASH1 + EGF (10.47 ± 0.48), and HASH1 - EGF (11.04 ± 0.31) were statistically different (Anova, p=0.02) at 40 mV (Figure 16). The post hoc test also demonstrated a statistical increase of current within the HASH1 - EGF treated group compared to the - EGF treated group (Bonferroni, p=0.016). There was also a statistically significant difference held at 0 mV (Anova, p=0.02) between the - EGF and the HASH1 - EGF treated groups (Bonferroni, p=0.03) (Figure 17). In contrast, there was no statistical differences in peak amplitudes observed at 20 mV (Anova, p=0.36) (Figure 18). Within the HASH1 + EGF treated group, there was an NSPC that had inward currents similar to a neuron (Figure 7 and Figure 19 A and B).

In the HASH1 + EGF treated cell with neuron properties, the inward current began when held at 0 mV (Figure 19 B), whereas, in the DRG neuron the inward current

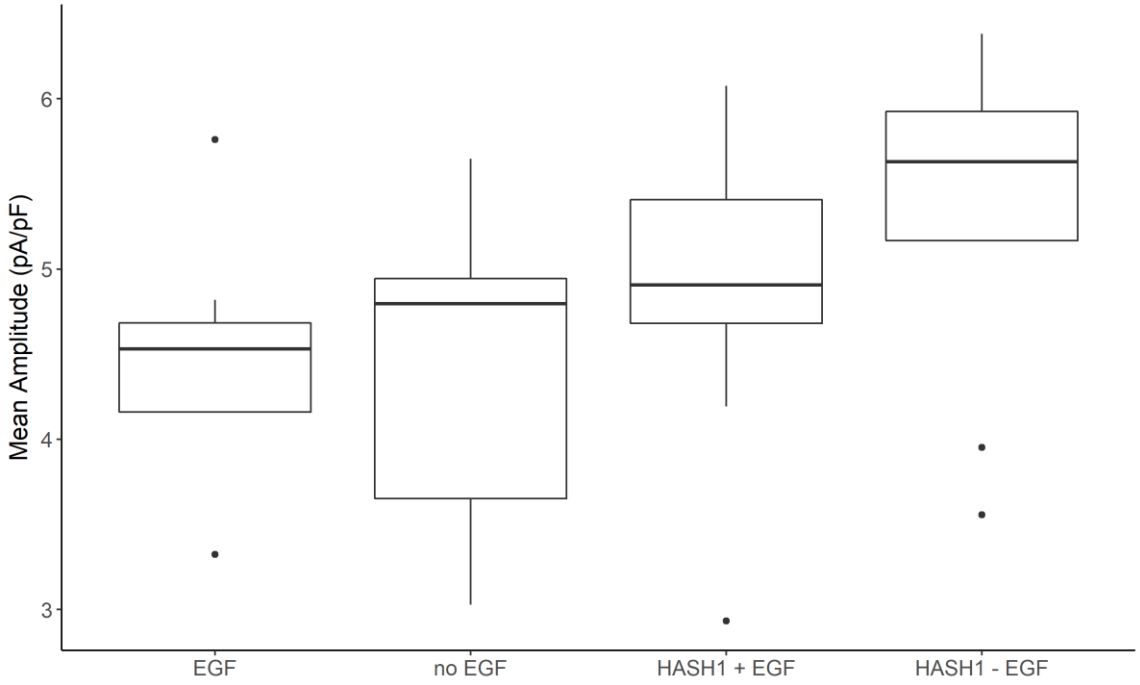

Figure 14. Mean amplitudes of NSPCs after one week of treatment at 0 mV. The mean amplitudes (pA/pF) of NSPCs grown with HASH1 ±EGF for one week *in vitro* between 13 ms to 43 ms of the electrophysiological recording are shown. The mean currents at 0 mV were not statistically different between groups (Anova, n=9, p=0.1).

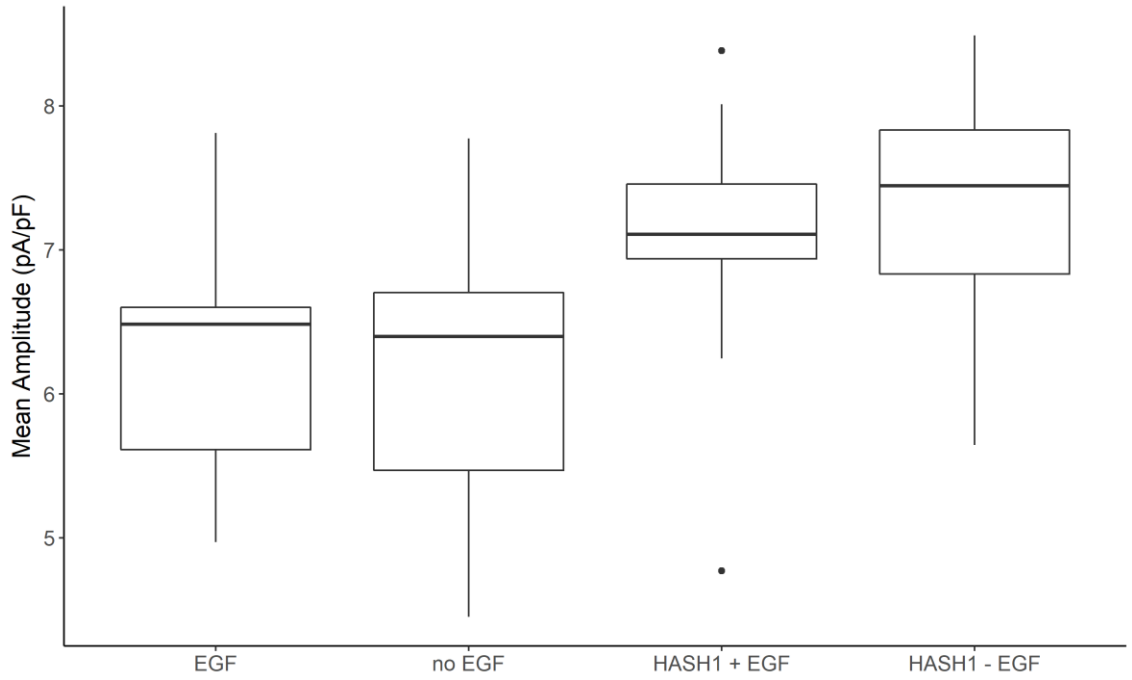

Figure 15. Mean amplitudes of NSPCs after one week of treatment at 20 mV. The mean amplitudes (pA/pF) of NSPCs grown with HASH1 ± EGF *in* vitro for one week between 13 ms and 43 ms of the electrophysiological recording are shown. The mean amplitudes were statistically different between groups (Anova, n=9, p=0.04); however, the Bonferroni post hoc test did not demonstrate any statistical differences.

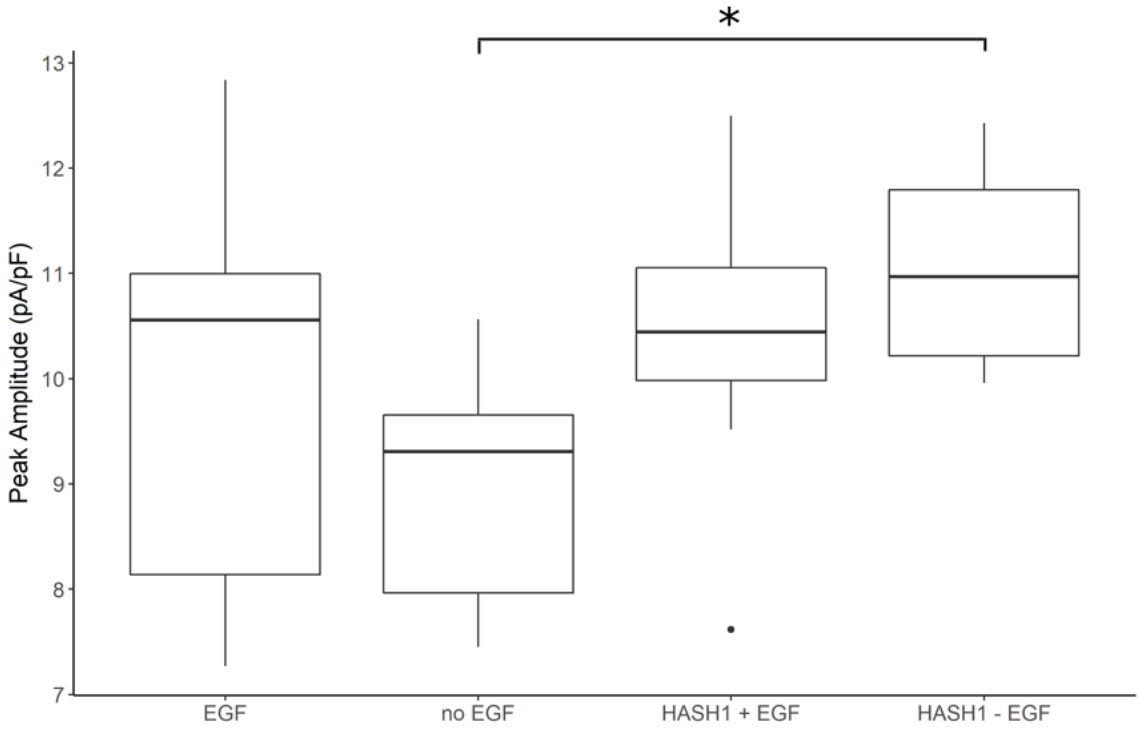

Figure 16. Peak amplitudes of NSPCs after one week of treatment at 40 mV. The peak amplitudes (pA/pF) of NSPCs grown with HASH1 ±EGF *in vitro* between13 ms to 43 ms of the electrophysiological recording are shown. The peak currents were statistically different between groups (Anova, n=9, p=0.02) and the post hoc demonstrated a difference in mean currents between the - EGF and the HASH1 - EGF treated groups (Bonferroni, p=0.02) indicated by the asterisk.

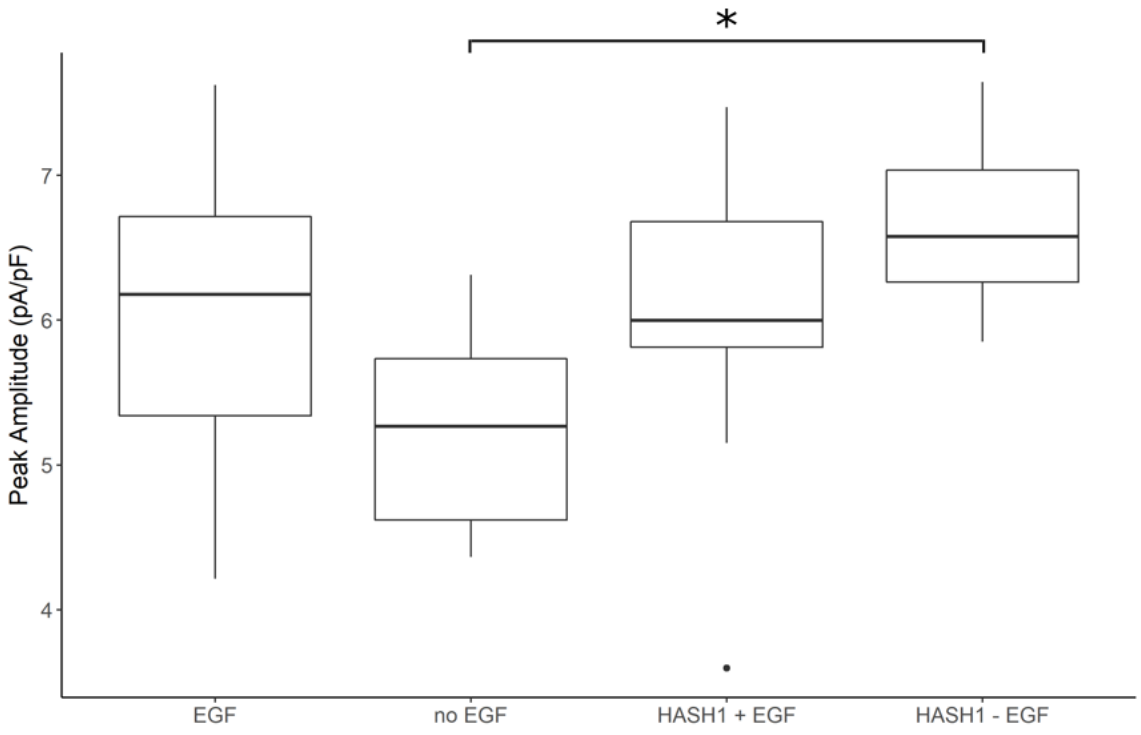

Figure 17. Peak amplitudes of NSPCs after one week of treatment at 0 mV The peak amplitudes (pA/pF) of NSPCs grown with HASH1 ± EGF *in vitro* for one week between 13 ms to 43 ms of the electrophysiological recording are shown. The peak currents were statistically different between groups (Anova, n=9, p=0.03) and the post hoc demonstrated a difference in mean currents between the - EGF and the HASH1 - EGF treated groups (Bonferroni, p=0.02) indicated by the asterisk.

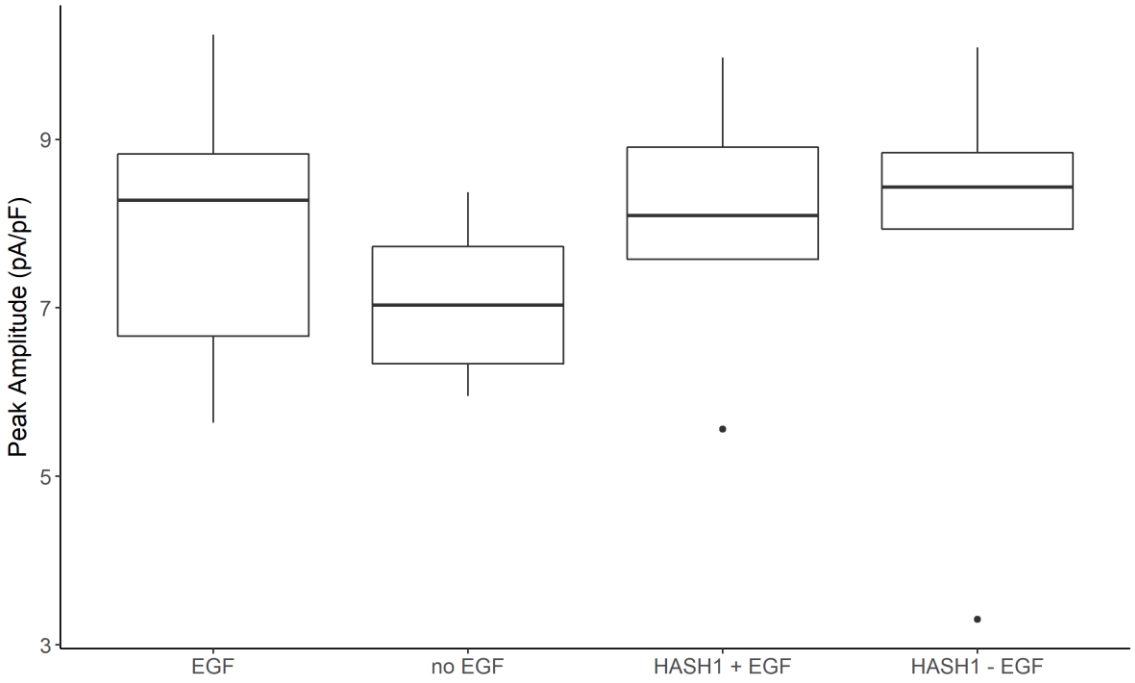

Figure 18. Peak amplitudes of NSPCs after one week of treatment at 20 mV. The peak amplitudes (pA/pF) of NSPCs grown for one week with HASH1 ±EGF *in vitro* between 13 ms to 43 ms of the electrophysiological recordings are shown. The peak currents at 20 mV were not statistically different between groups (Anova, n=9, p=0.36).

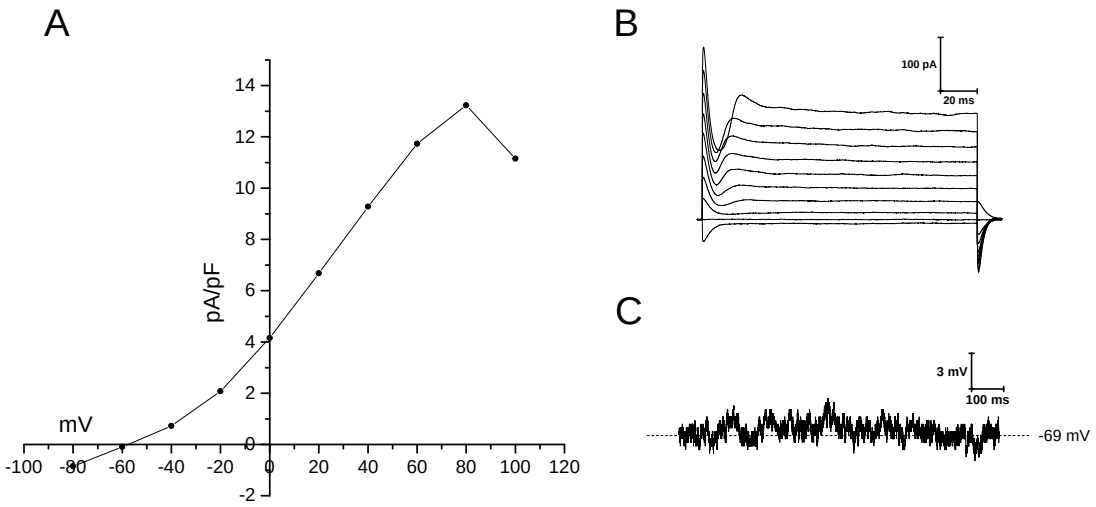

Figure 19. Patch-clamp electrophysiology of an NSPC treated for one week with HASH1 + EGF. The current-density (pA/pF) versus voltage (mV) plot a NSPC grown for one week *in vitro* with HASH1 + EGF at 20 ms into the recording (A), the current (pA) from the voltage-clamp recording (B), and the resting membrane voltage (mV) (C) is shown.

began when held at 20 mV (Figure 7 B). In addition, the inward current were sharper in the DRG neuron, the inward current was less sharp in the HASH1 + EGF treated cell and had lower whole cell currents (Figures 7 B and 19 A and B). The resting membrane voltage of the HASH1 + EGF treated NSPC was approximately -68.5 mV and had membrane voltage fluctuations up to 5 mV (Figure 19 C).

3.3.2 Immunocytochemistry

Less than 10% of NSPCs grown in +EGF stained positive NF and the cells that did stain positive had low fluorescence intensities (Figure 20 A). NSPCs grown in - EGF stained positive for NF with 80 - 90% of cells staining positive and had a brighter fluorescence intensities compared to the EGF group (Figure 20 B). Both groups that were treated with HASH1 stained positive for NF with 80 - 90% staining positive and had a brighter fluorescence compared to the EGF group (Figure 20 C and D). While the cells were positive for NF, it was localized near the nucleus and not in projections off the cell as it would be expected in a neuron (Figure 6).

3.4 Two week HASH1 driving experiments

3.4.1 Electrophysiology

To test if more time was needed for neural differentiation, NSPCs were grown for two weeks in the presence and absence of HASH1 and EGF. The mean (±SEM) Cm (pF) for NSPCs treated for two weeks with EGF (11.30 ± 0.14, n=9), - EGF (11.03 ± 0.09, n=9), HASH1 + EGF (11.35 ± 0.13, n=11), and HASH1 - EGF (11.58 ± 0.34, n=10)

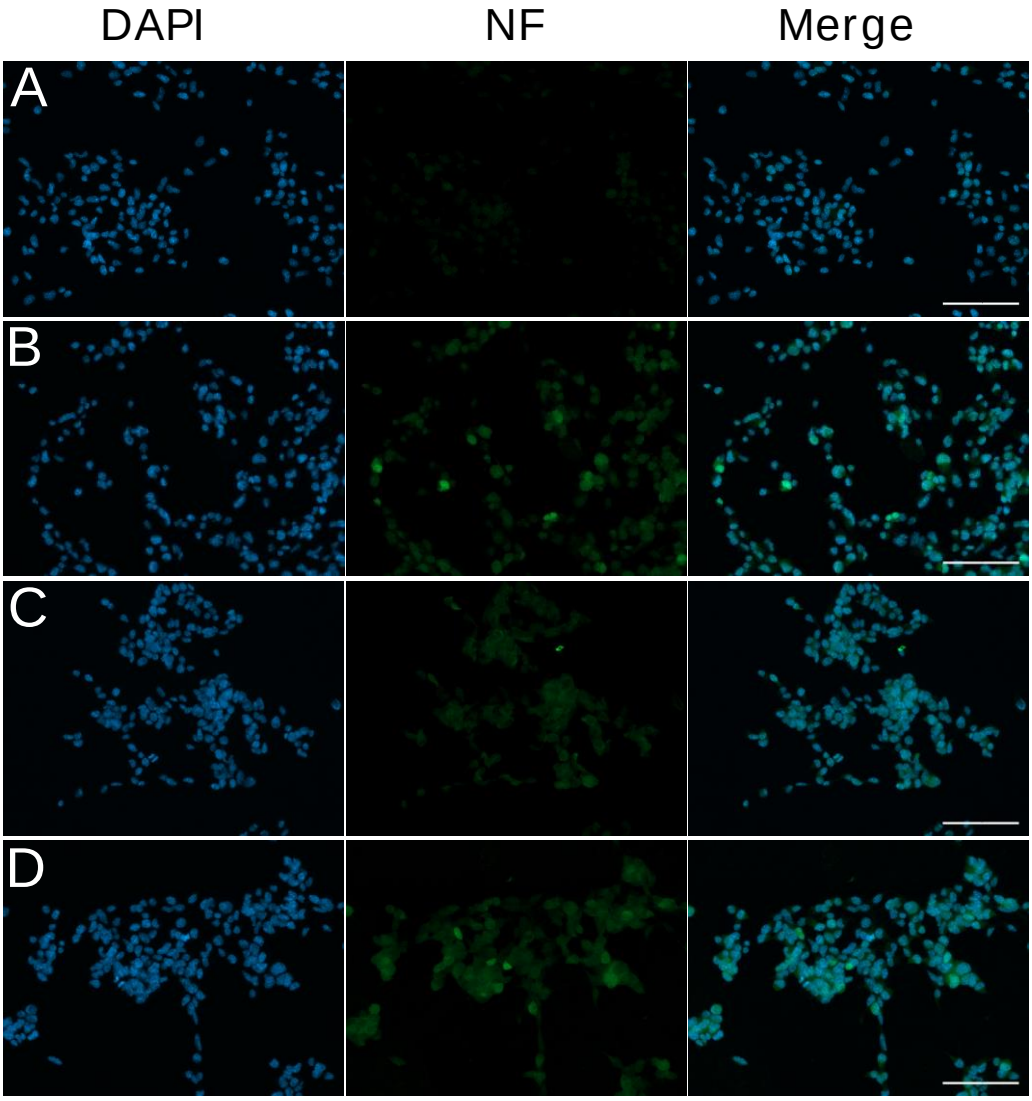

Figure 20. Immunocytochemistry of NSPCs treated for one week NSPCs were grown in vitro for one week in EGF (A), - EGF (B), HASH1 + EGF (C), and HASH1 - EGF (D). Immunocytochemistry was done for neurofilament (NF) (green) and the nuclear stain DAPI (blue). Images are at 200X and the scale bar is 100 µm.

were not statistically different (Anova, p=0.32) (Figure 21). The mean cell sizes for cells treated for two weeks were similar to those of the cells treated for one week (Figure 8).

In the current-density (pA/pF) versus voltage (mV) plots of cells treated for two weeks at 50 ms into the recording, the HASH1 + EGF had the lowest current-density compared to the other groups (Figure 22). This observation is contrary to currents observed when cells were treated for one week (Figure 9). The mean (± SEM) current-densities (pA/pF) of NSPCs at 20 mV 50 ms into the recording treated with EGF (7.85 ± 0.44), - EGF (7.31 ± 0.39), HASH1 + EGF (6.13 ± 0.25) and HASH1 - EGF (7.45 ± 0.43) were statistically different (Anova, p=0.003) (Figure 23). The post hoc Bonferroni test showed that the HASH1 + EGF group was statistically lower from all treatment groups (EGF p=0.032, no EGF p=0.045, and HASH1 - EGF p=0.022). After two weeks of treatment, the HASH1 + EGF group had 1.3-fold decrease in whole cell currents. There was also inward current immediately following the capacitive transient held at voltages higher than 0 mV; however, the inward current was observed less often than the 23 seen at one week with 1 NSPC in the EGF group, 1 NSPC in the - EGF group, 6 NSPCs in the HASH1 + EGF group, and 2 NSPCs in the HASH1 - EGF group.

The total current amplitude over the duration of the recording at various potentials varied. The transient inward current was observed between 13 ms and 43 ms, after the capacitive transient. To observe the characteristics of this decrease in current, the anti-peak (min), mean, and peak (max) amplitudes (pA/pF) were taken for NSPCs held at 0 mV, 20 mV and the 40 mV in the time interval of 13 ms to 43 ms. Although all voltages are in the biological range, the focus is on the 40 mV.

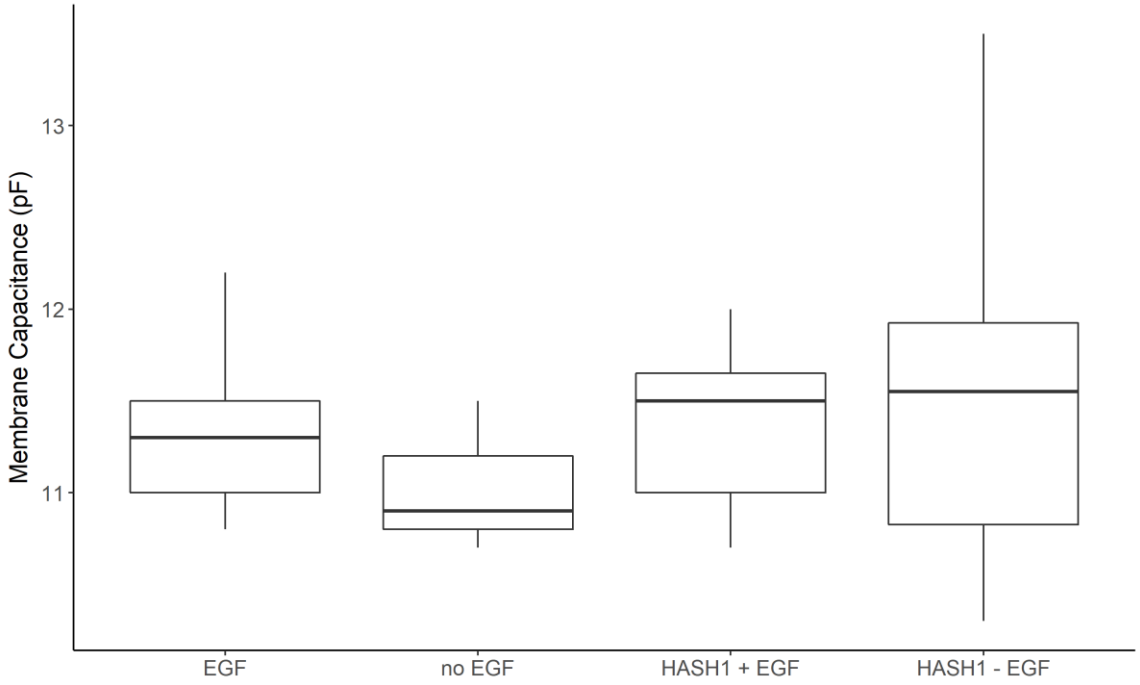

Figure 21. Membrane capacitances of NSPCs after two weeks of treatment. The membrane capacitances (pF) from cells grown with HASH1 ±EGF *in* vitro for two weeks are shown (EGF n=9, no EGF n=9, HASH1 + EGF n=11, and HASH1 - EGF n=10). There were no statistical differences in membrane capacitances at two weeks between groups (Anova, p=0.32).

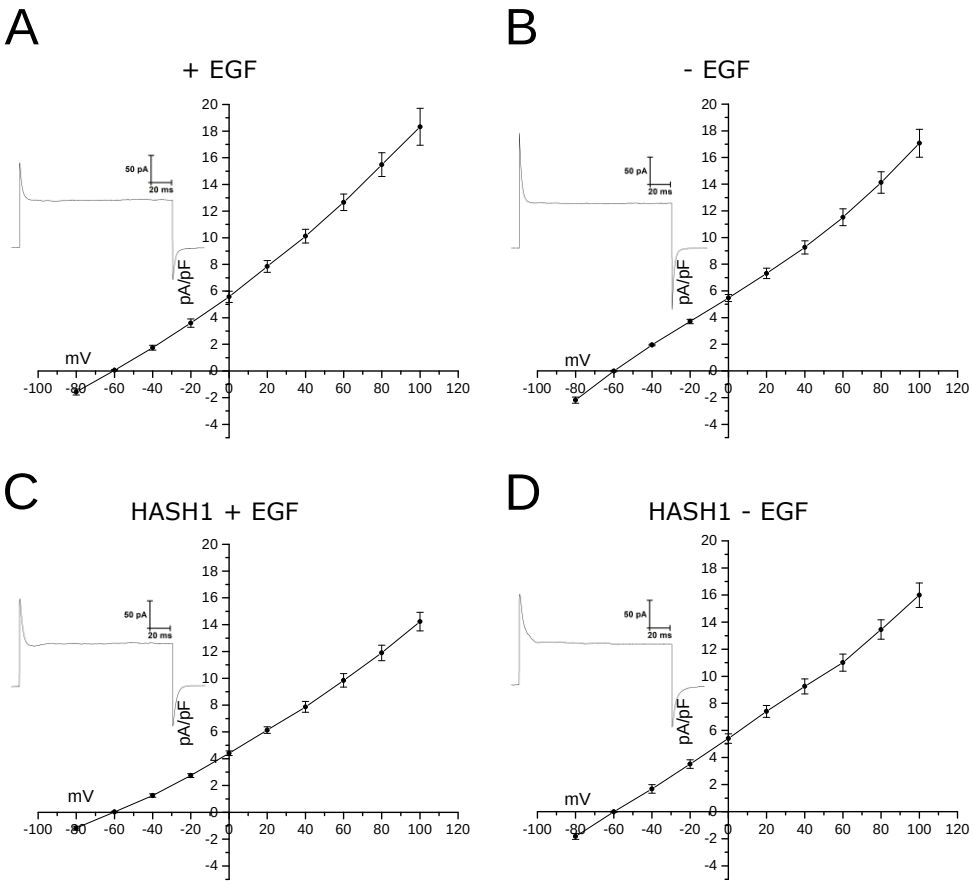

Figure 22. Patch-clamp electrophysiology of NSPCs after two weeks of treatment. The mean (± SEM) current-densities (pA/pF) versus voltage (mV) plots for NSPCs grown *in vitro* for two weeks with EGF (A), - EGF (B), HASH1 + EGF (C), and HASH1 - EGF (D) are shown (EGF n=9, no EGF n=9, HASH1 + EGF n=11, and HASH1 - EGF n=10). A representative electrophysiological current trace at 20 mV is inserted in each plot.

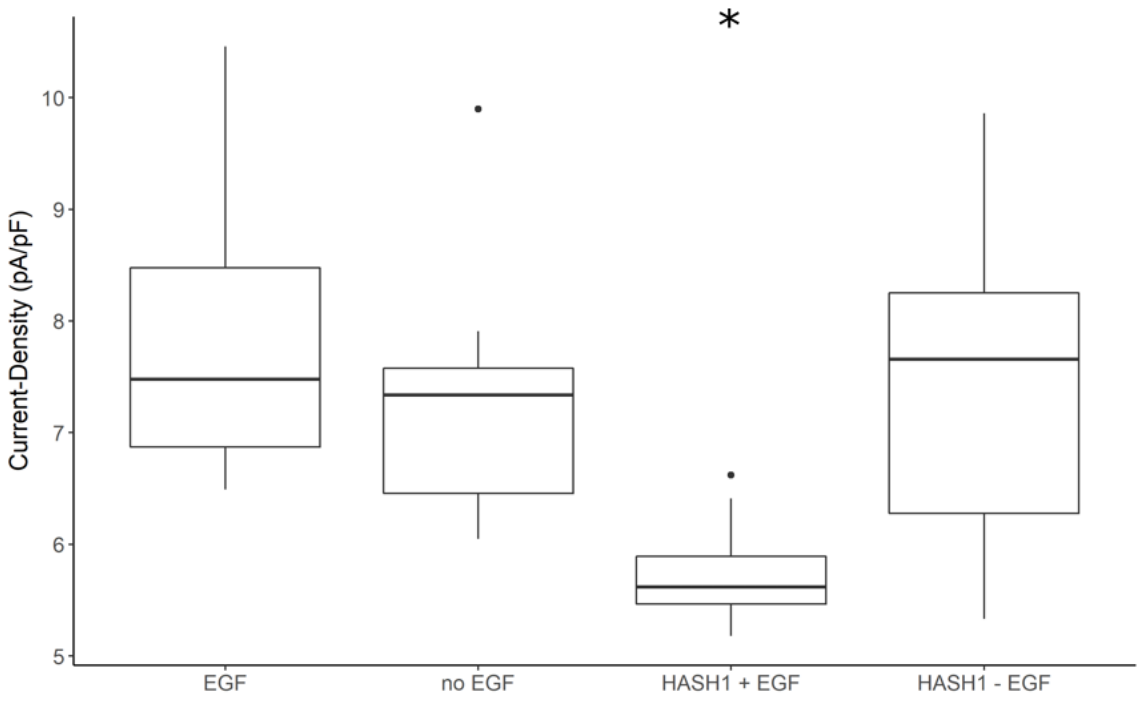

Figure 23. Current-densities of NSPCs grown for 2 weeks at 20 mV. The current-densities (pA/pF) at 50 ms into the electrophysiological recording of NSPCs treat with HASH1 ±EGF for two weeks *in vitro* are shown (EGF n=9, - EGF n=9, HASH1 + EGF n=11, and HASH1 - EGF n=10). The current-densities at 20 mV were statistically different between groups (Anova, p= 0.003) and the Bonferroni post hoc test demonstrated that the HASH1 + EGF was lower than all other treatment groups (EGF p=0.032, no EGF p=0.045, and HASH1 - EGF p=0.022) indicated by the asterisk.

The anti-peak was observed to try to capture the inward current following the capacitive transient. The mean (± SEM) of the anti-peak amplitudes (pA/pF) of NSPCs treated with EGF (9.76 ± 0.54), without EGF (9.23 ± 0.50), HASH1 + EGF (7.44 ± 0.43), and HASH1 - EGF (9.11 ± 0.55) were statistically different (Anova, p=0.01) at 40 mV (Figure 24). The post hoc test demonstrated that the HASH1 + EGF group was statistically lower than the EGF treated group (Bonferroni, p=0.01). The same was observed at lower potentials; there was a statistical difference at 0 m V (Anova, p=0.02) with the EGF and HASH1 + EGF groups different (Bonferroni, p=0.05) (Figure 25) and a statistical difference at 20 mV (Anova, p=0.012) with the EGF and HASH1 + EGF groups different (Bonferroni, p=0.02) (Figure 26). The means (± SEM) of the mean amplitudes (pA/pF) of NSPCs treated with EGF (10.23 ± 0.51), - EGF (9.49 ± 0.50), HASH1 + EGF (7.90 ± 0.42), and HASH1 - EGF (9.60 ± 0.54) were statistically different (Anova, p=0.01) at 40 mV (Figure 27). The post hoc test showed that the HASH1 + EGF treated group was statistically different than the EGF treated group (Bonferroni, p=0.01). The means were also statistically different when at 0 mV (Anova, p= 0.015) (Figure 28) and at 20 mV (Anova, p=0.018) (Figure 29).

The post hoc test also demonstrated a statistical difference between the EGF and the HASH1 + EGF treated groups at 0 mV (Bonferroni, p=0.018) and at 20 mV (Bonferroni, p=0.046). The mean (± SEM) of the peak amplitudes (pA/pF) of NSPCs treated with EGF (11.24 ± 0.53), without EGF (10.69 ± 0.51), HASH1 + EGF (9.08 ± 0.39), and HASH1 - EGF (11.24 ± 0.69) were statistically different form each other (Anova, p=0.016) at 40 mV (Figure 30). The post hoc test showed a statistical difference

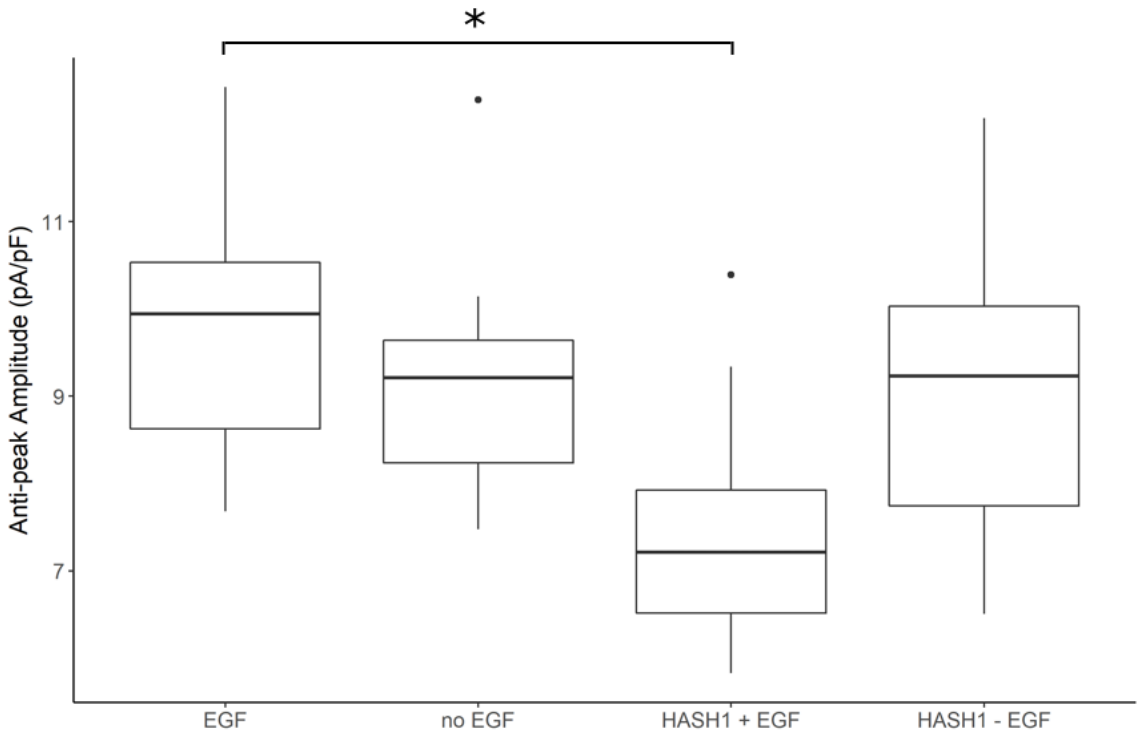

Figure 24. Anti-peak amplitudes of NSPCs after 2 weeks of treatment at 40 mV. The anti-peak amplitudes (pA/pF) of NSPCs grown with HASH1 ± EGF for one week in vitro between 13 ms to 43s of the electrophysiological recording are shown (EGF n=9, -EGF n=9, HASH1 + EGF n=11, and HASH1 - EGF n=10). The anti-peak currents at 40 mV were statistically different between groups (Anova, p=0.01) and the Bonferroni post hoc test demonstrated a difference between the EGF and the HASH1 + EGF treated groups (p=0.013) indicated by the asterisk.

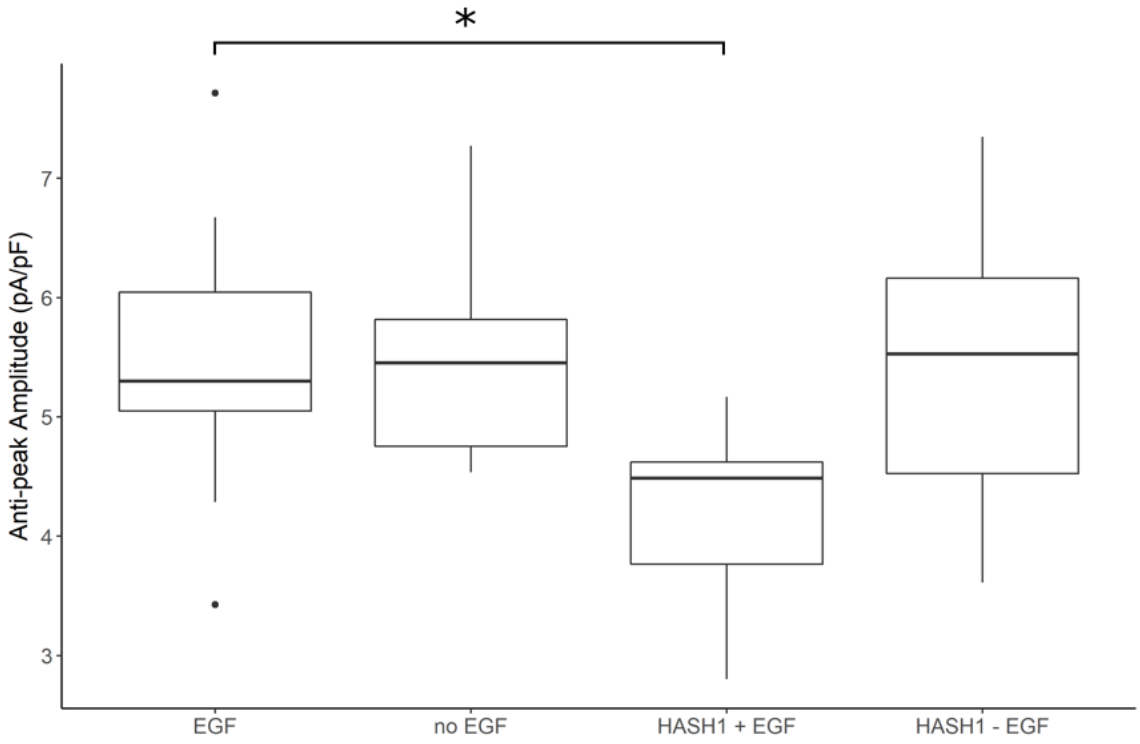

Figure 25. Anti-peak amplitudes of NSPCs after 2 weeks of treatment at 0 mV. The anti-peak amplitudes (pA/pF) of NSPCs grown with HASH1 ± EGF for two weeks *in vitro* between 13 ms to 43 ms of the electrophysiological recording are shown (EGF n=9, no EGF n=9, HASH1 + EGF n=11, and HASH1 - EGF n=10). The anti-peak currents at 0 mV were statistically different between groups (Anova, p=0.02) and the Bonferroni post hoc test demonstrated a difference between the EGF and HASH1 + EGF treated groups (p=0.05) indicated by the asterisk.

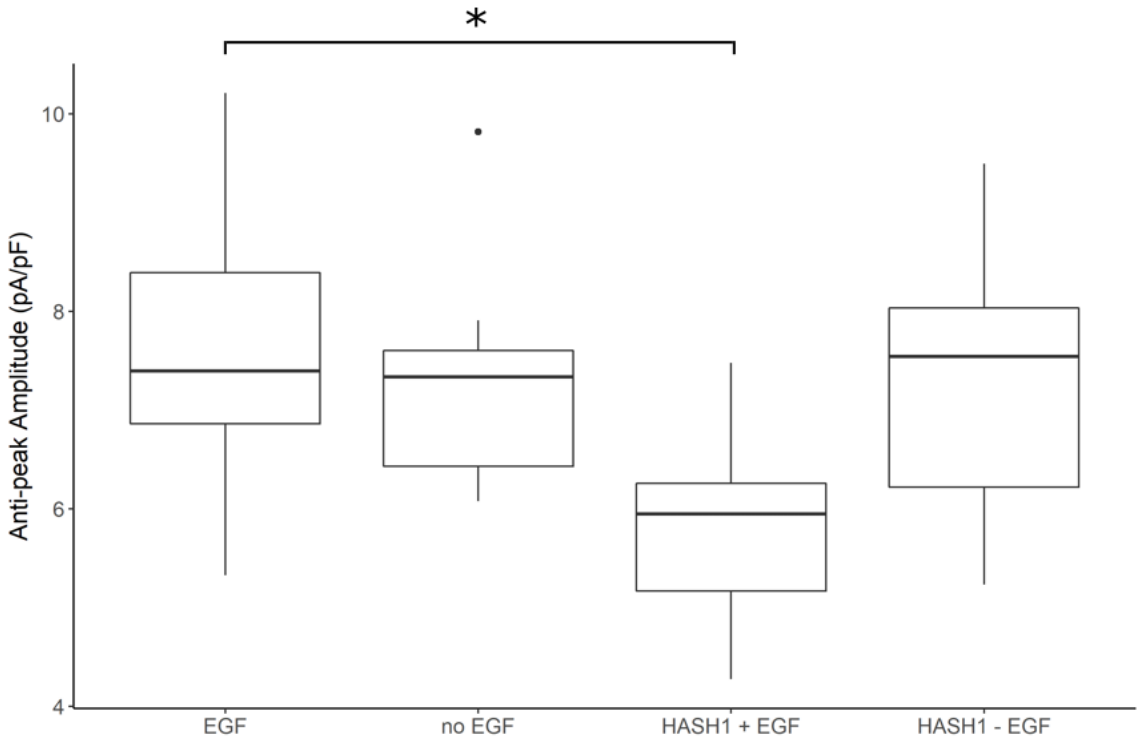

Figure 26. Anti-peak amplitudes of NSPCs after 2 weeks of treatment at 20 mV. The anti-peak amplitudes (pA/pF) of NSPCs grown with HASH1 ±EGF for one week in vitro between 13 ms to 43s of the electrophysiological recording are shown (EGF n=9, no EGF n=9, HASH1 + EGF n=11, and HASH1 - EGF n=10). The anti-peak currents at 20 mV were statistically different between groups (Anova, p=0.02) and the Bonferroni post hoc test demonstrated a difference between the EGF and the HASH1 + EGF treated groups (p=0.02) indicated by the asterisk.

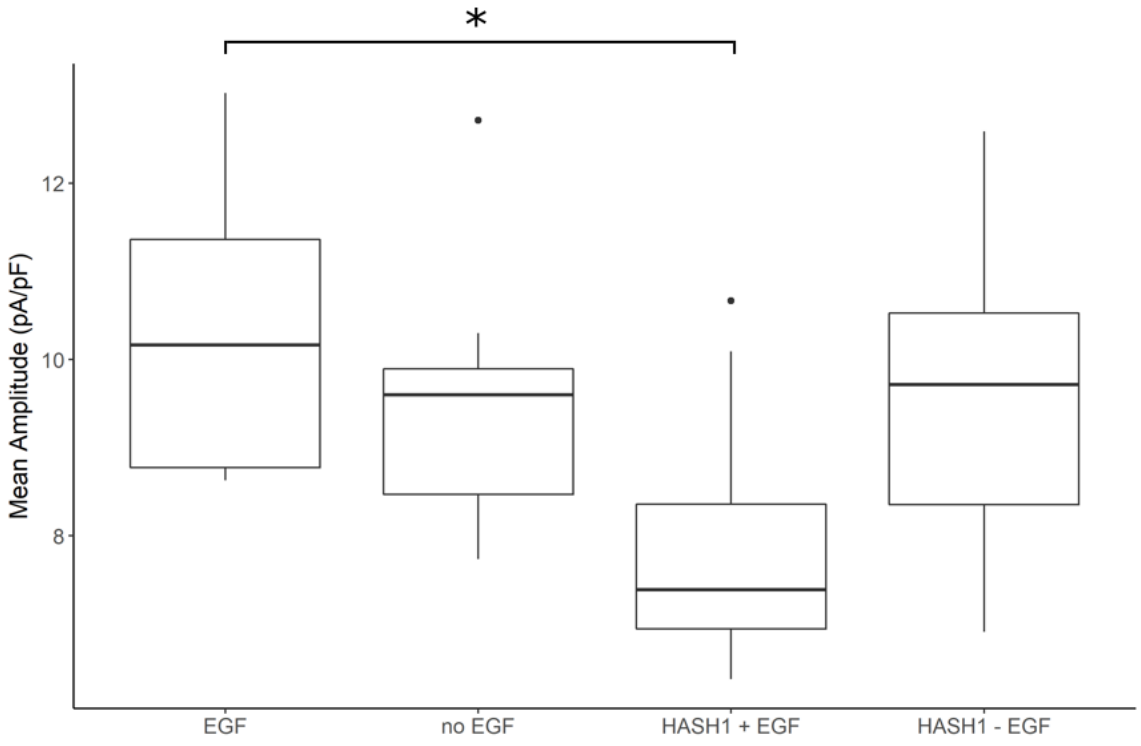

Figure 27. Mean amplitudes of NSPCs after 2 weeks of treatment at 40 mV. The anti-peak amplitudes (pA/pF) of NSPCs grown with HASH1 ± EGF for one week in vitro between 13 ms to 43s of the electrophysiological recording are shown (EGF n=9, no EGF n=9, HASH1 + EGF n=11, and HASH1 - EGF n=10). The mean currents were statistically different (Anova, p=0.01) and the Bonferroni post hoc test demonstrated a difference between the EGF and the HASH1 + EGF treated groups (p=0.01) indicated by the asterisk.

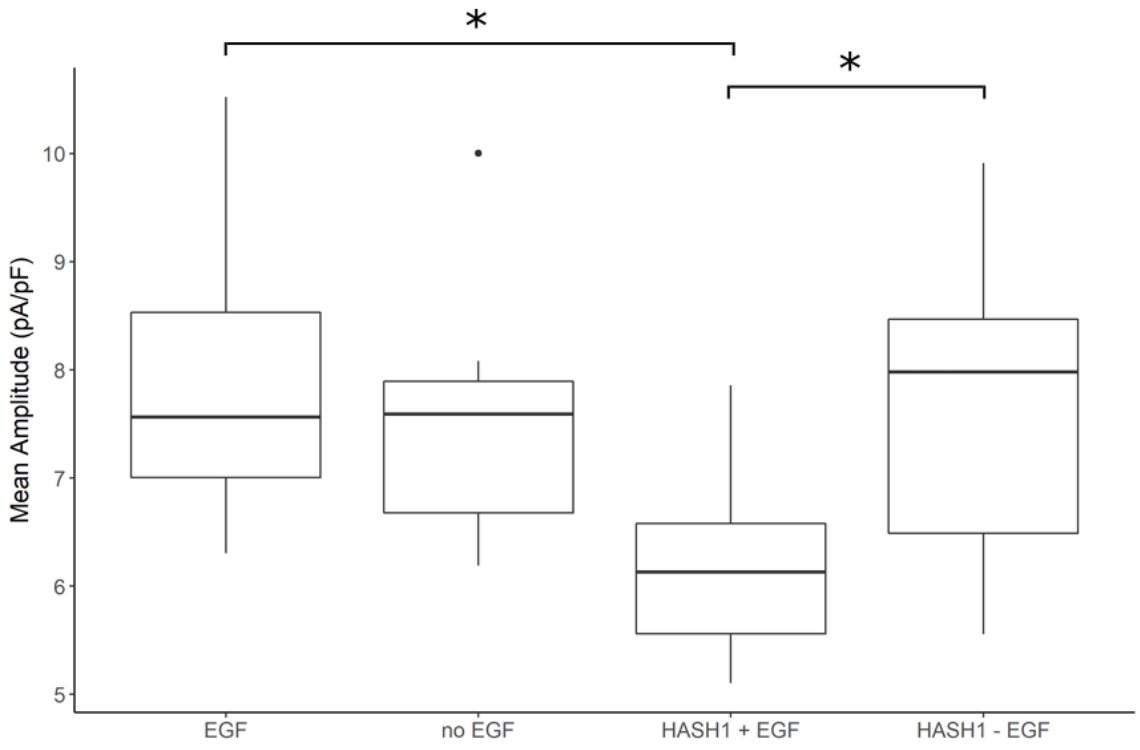

Figure 28. Mean amplitudes of NSPCs after one week of treatment at 0 mV. The mean amplitudes (pA/pF) of NSPCs grown with HASH1 ±EGF for one week in vitro between13 ms to 43 ms of the electrophysiological recording are shown (EGF n=9, no EGF n=9, HASH1 + EGF n=11, and HASH1 - EGF n=10). The mean currents at 0 mV were statistically different between groups (Anova, p=0.015) and the Bonferroni post hoc test demonstrated a difference between the EGF and HASH1 + EGF treated groups (p=0.046) and a difference between the HASH1 + EGF and the HASH1 - EGF treated groups (p=0.045).

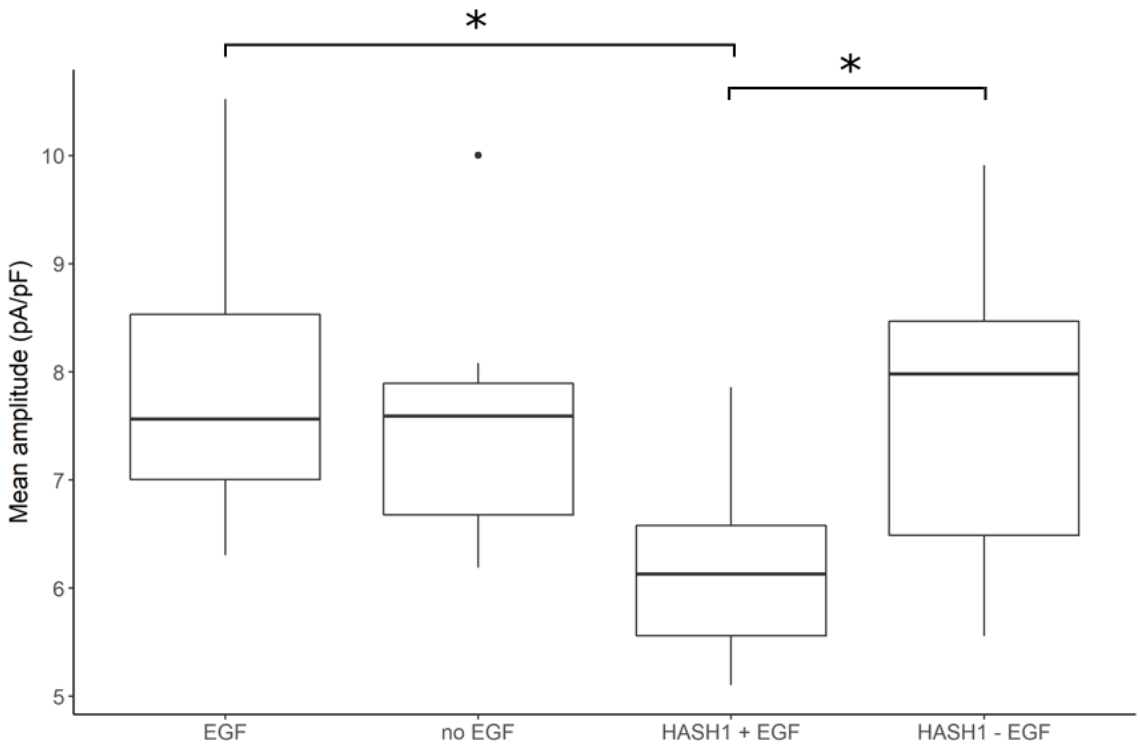

Figure 29. Mean amplitudes of NSPCs after 2 weeks of treatment at 20 mV The mean amplitudes (pA/pF) of NSPCs grown with HASH1 ±EGF for two weeks in vitro between13 ms to 43 ms in the electrophysiological recording are shown (EGF n=9, -EGF n=9, HASH1 + EGF n=11, and HASH1 - EGF n=10). The mean currents were statistically different between groups (Anova, p=0.01) and the Bonferroni post host test demonstrated a difference between the EGF and the HASH1 + EGF treated groups (p=0.018) and a difference between the HASH1 + EGF and the HASH1 - EGF treated groups (p=0.047) indicated by the asterisk.

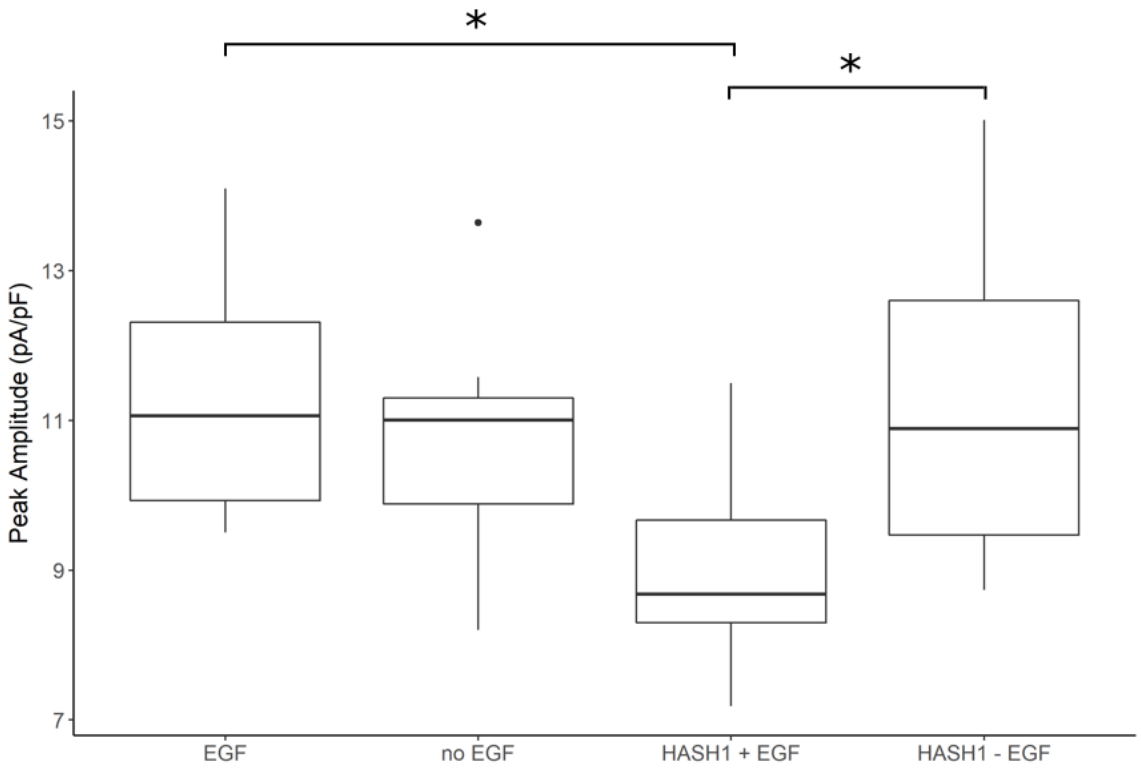

Figure 30. Peak amplitudes of NSPCs after two weeks of treatment at 40 mV. The peak amplitudes (pA/pF) of NSPCs grown with HASH1 ± EGF for one week in vitro between 13 ms to 43 ms of the electrophysiological recording are shown(EGF n=9, - EGF n=9, HASH1 + EGF n=11, and HASH1 - EGF n=10). The peak currents at 40 mV were statistically different between groups (Anova, p=0.016) and the Bonferroni post hoc test demonstrated a difference between the EGF and the HASH1 + EGF treated groups (p=0.04) and a difference between the HASH1 + EGF and the HASH1 - EGF treated groups (p=0.03).

between the EGF and HASH1 + EGF treated groups (Bonferroni, p=0.04) and between the HASH1 + EGF and HASH1 - EGF treated groups (Bonferroni, p=0.03). In most recordings, the peak amplitude occurred at 13 ms during the decline of the capacitive transient; however, there was outward current following the inward current after the capacitive transient that occurred between 17 ms and 25 ms in the recordings for 1 NSPC in the EGF group, 1 in the HASH1 + EGF groups and 1 in the HASH1 - EGF treated groups. The means of the peak amplitude when held at 0 mV were also statistically different (Anova, p=0.026) and the post hoc test demonstrated that the HASH1 + EGF and the HASH1 - EGF groups were different (Bonferroni, p=0.016) (Figure 31). The same was observed at 20 mV, the means were statistically different (Anova, p=0.018) and a difference between the HASH1 + EGF and the HASH1 - EGF treated groups (Bonferroni, p=0.02) (Figure 32). Overall, there was a 1.3-fold decrease in whole cell currents of NSPCs treated with HASH1 and EGF.

The observations from the electrophysiology from the two week experiment were different than the one week experiment. In all measures of current in cells grown for two weeks, the HASH1 + EGF treated group had lower mean currents while the other groups remained similar to the EGF group. In the - EGF treated group, there was one NSPC that could respond to glutamate (Figure 33 D). During the voltage-clamp, there were no inward current at higher voltages, but there was small inward and outward currents observed at -20 mV and 0 mV (Figure 33 A and B). When 0.1 nA was injected into this cell during a current-clamp, the membrane voltage was brought from -55 mV to -5 mV and there were fluctuations between -10 mV and -5 mV, demonstrating an unstable resting membrane potential (Figure 33 C).

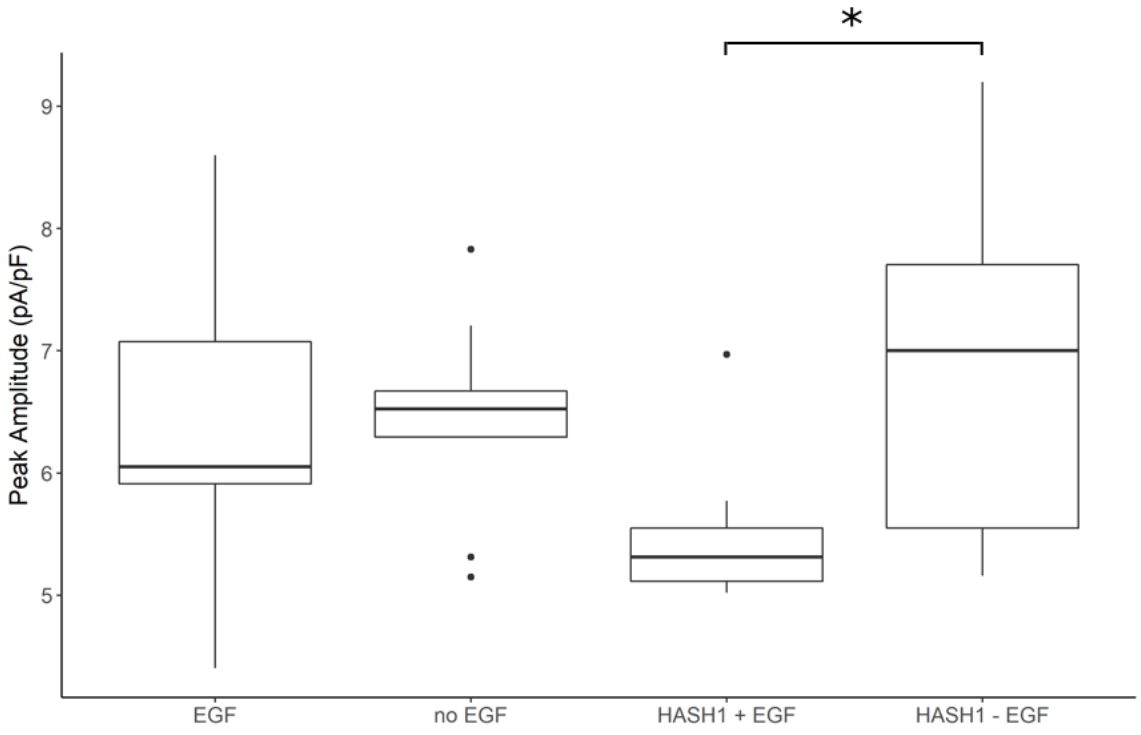

Figure 31. Peak amplitudes of NSPCs after 2 weeks of treatment at 0 mV. The peak amplitudes (pA/pF) of NSPCs grown with HASH1 ±EGF for two weeks in vitro between 13 ms to 43 ms of the electrophysiological recording are shown (EGF n=9, - EGF n=9, HASH1 + EGF n=11, and HASH1 - EGF n=10). The peak currents at 0 mV were statistically different between groups (Anova, p=0.03) and the Bonferroni post hoc test demonstrated a difference between the HASH1 + EGF and the HASH1 - EGF treated groups (p=0.02).

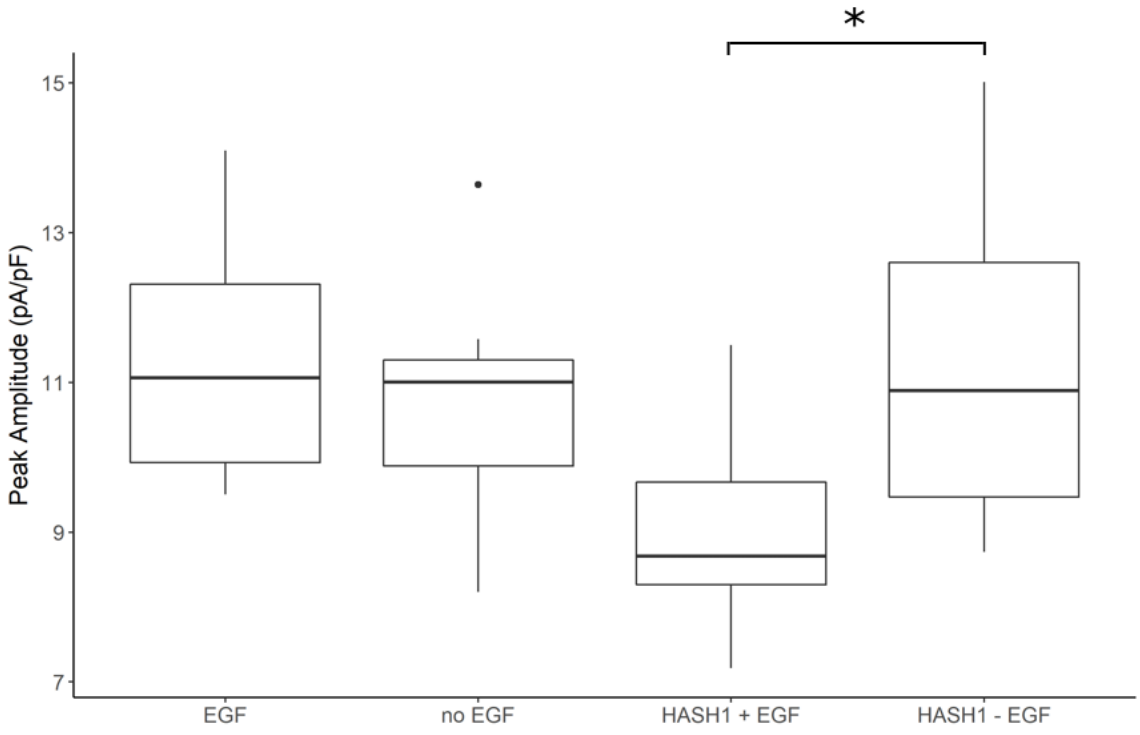

Figure 32. Peak amplitudes of NSPCs after 2 weeks of treatment at 20 mV. The peak amplitudes (pA/pF) of NSPCs grown with HASH1 ± EGF for two weeks in vitro between13 ms to 43 ms of the electrophysiological recording are shown (EGF n=9,-EGF n=9, HASH1 + EGF n=11, and HASH1 - EGF n=10). The peak currents at 20m mV were statistically different between groups (Anova, p=0.018) and the Bonferroni post hoc test demonstrated a difference between the HASH1 + EGF and the HASH1 - EGF treated groups (p=0.02).

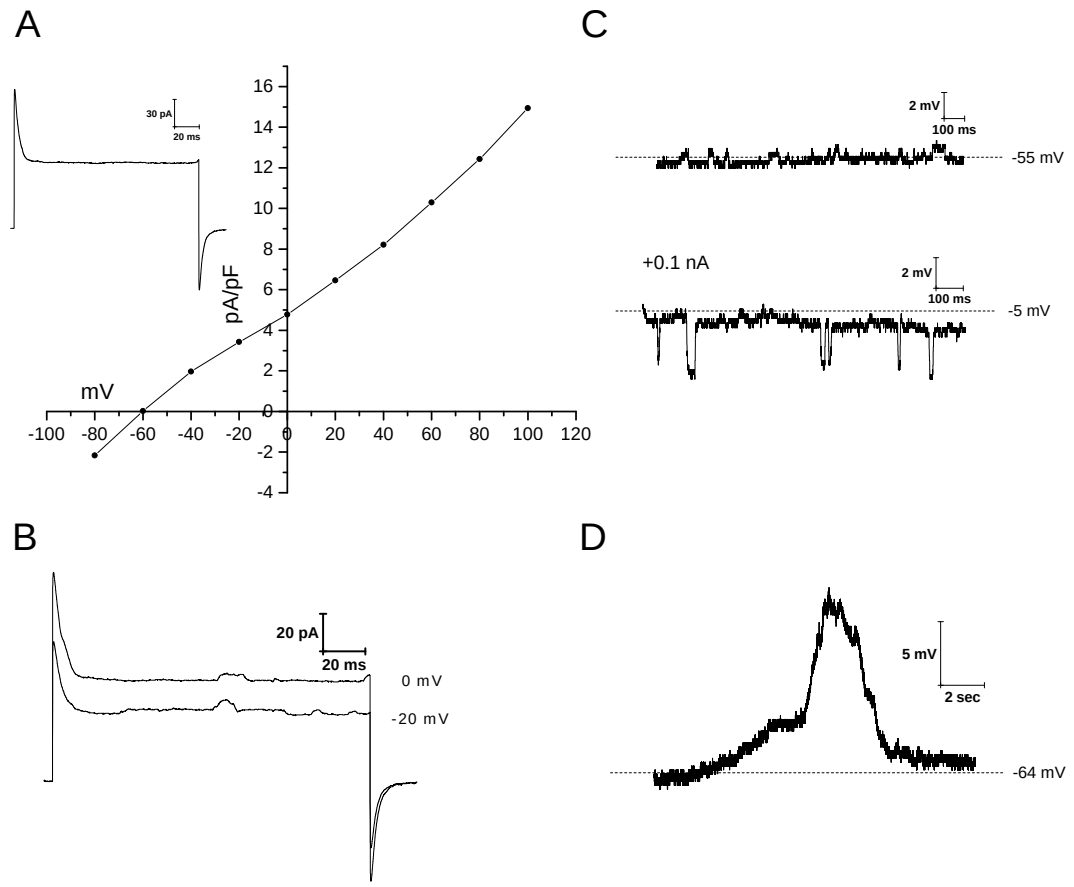

Figure 33. Patch-clamp electrophysiology of an NSPC treated for 2 weeks - EGF. The current-density (pA/pF) versus voltage (mV) plot of an NSPC grown in vitro without EGF with a representative current (pA) trace at 20 mV (A), the current (pA) when held at -20 mV and 0 mV (B), the membrane voltage (mV) at rest (top) and when the current is clamped at 0.1 nA (C), and the membrane voltage when glutamate is added (D) is shown.

3.3.2. Immunocytochemistry

Because the cells were very confluent (80 - 100%) after 12 days, the stains were done on day 12 rather than day 14. There were less than 1% of cells that stained positive for NF in the EGF group and the fluorescence intensity was low (Figure 34 A). At least 90% of the cells in the - EGF group stained positive for NF and had a brighter fluorescence intensity compared to the EGF group (Figure 34 B). The HASH1 treated groups also stained positive for NF with 50-75% of the cells staining positive (Figure 34 C and D). The - EGF group appears to have the highest proportion of cells expressing NF. In most of the cells that stained positive for NF, the NF was localized close to the cell nucleus; however, a neurofilament can be seen in the 12 day HASH1 - EGF treated group (Figure 34 D top center). Immunocytochemistry was done on three biological replicates for the cells treated for 12 days. Growing the cells longer did not appear to increase the levels of NF; instead, they continued to proliferate.

To determine if the transient inward current following the capacitive transient was from voltage gated sodium channels, the sodium channel inhibitor tetrodotoxin (TTX) was added into the recording solution. When TTX was added to NSPCs grown (n=2) with EGF there was a 1.14-fold increase of current; however, washing with recording solution did not return the current to pre-treatment levels (Figure 35). Adding TTX to a NSPC treated for one week with HASH1 + EGF caused a 1.34-fold increase of current when held at 100 mV (Figure 36 A). Addition of TTX did not remove the inward current after the capacitive transient (Figure 36 B, C and D). Washing TTX off with

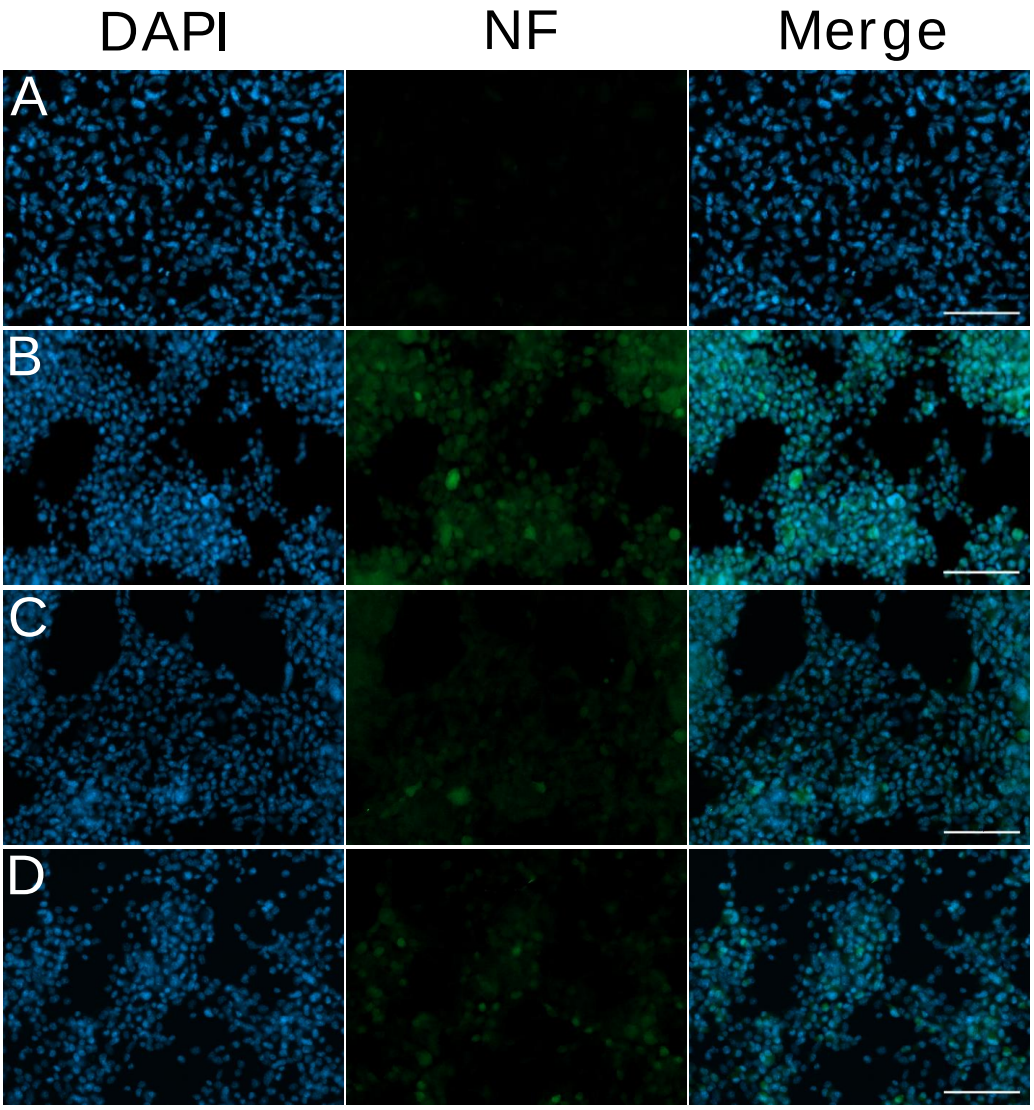

Figure 34. Immunocytochemistry of NSPCs treated for two weeks. NSPCs were grown for one week in vitro in EGF (A), - EGF (B), with HASH1 + EGF (C), and HASH1 - EGF (D). Immunocytochemistry was done for the neural marker neurofilament (green) and the nuclear stain DAPI (blue). Images are at 20X and the scale bar is 100 µm.

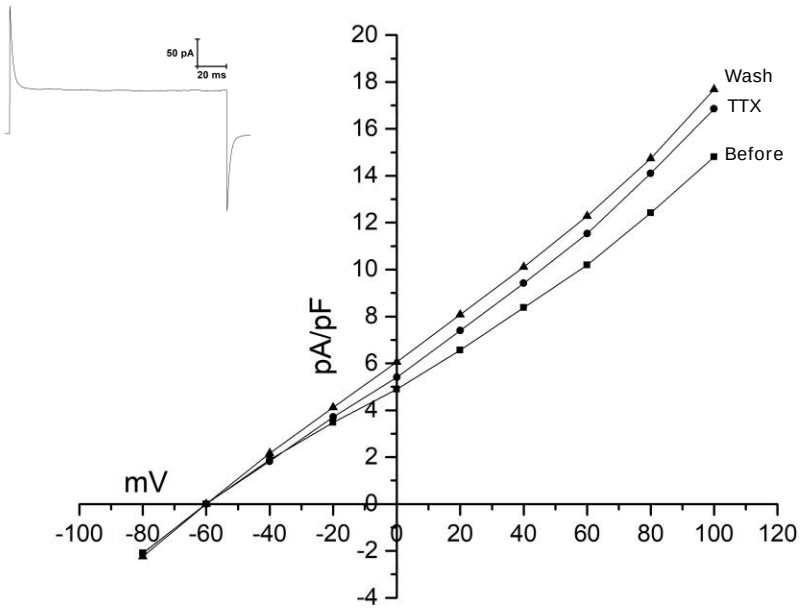

Figure 35. Sodium channel inhibitor on an NSPC. The current-density (pA/pF) versus voltage (mV) plot at 50 ms for an NSPC cultured with EGF for one week in vitro in ERS (before), TTX and a wash with ERS is shown.

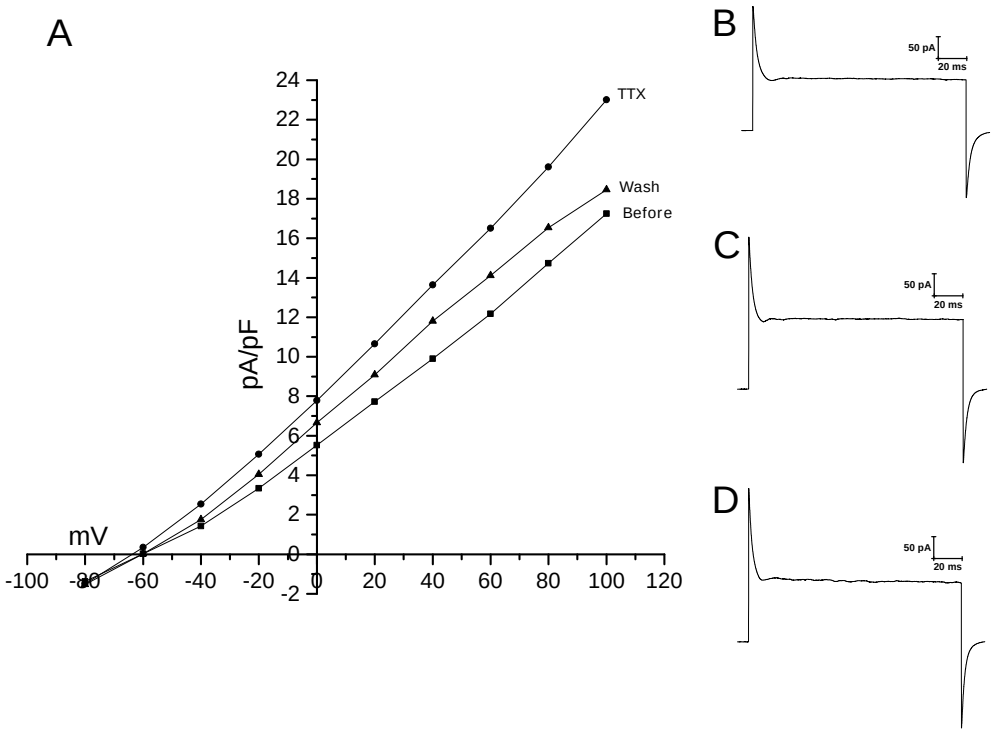

Figure 36. Sodium channel inhibitor on NSPC treated with HASH1 +EGF for one week. The current-density (pA/pF) versus voltage (mV) plot at 50 ms for an NSPC treated with HASH1 + EGF for one week in vitro in ERS (before), TTX and a wash with ERS is shown (A). The current (pA) of the NSPC when held at 20 mV in ERS (B), TTX (C), and wash with ERS (D).

recording solution removed most of the effect and the current decreased close to the initial recording (Figure 36 A).

3.5.1 Cadmium chloride

When CdCl was added to a NSPC treated with HASH1 + EGF for 2 weeks there was a 1.15-fold increase of current when held at 100 mV (Figure 37 A). Washing with recording solution did not return the current to pre-treatment levels (Figure 37 A). This NSPC had inward and outward currents (Figure 37 A); the addition of CdCl did not change the inward and outward currents (Figure 37 B, C, and D).

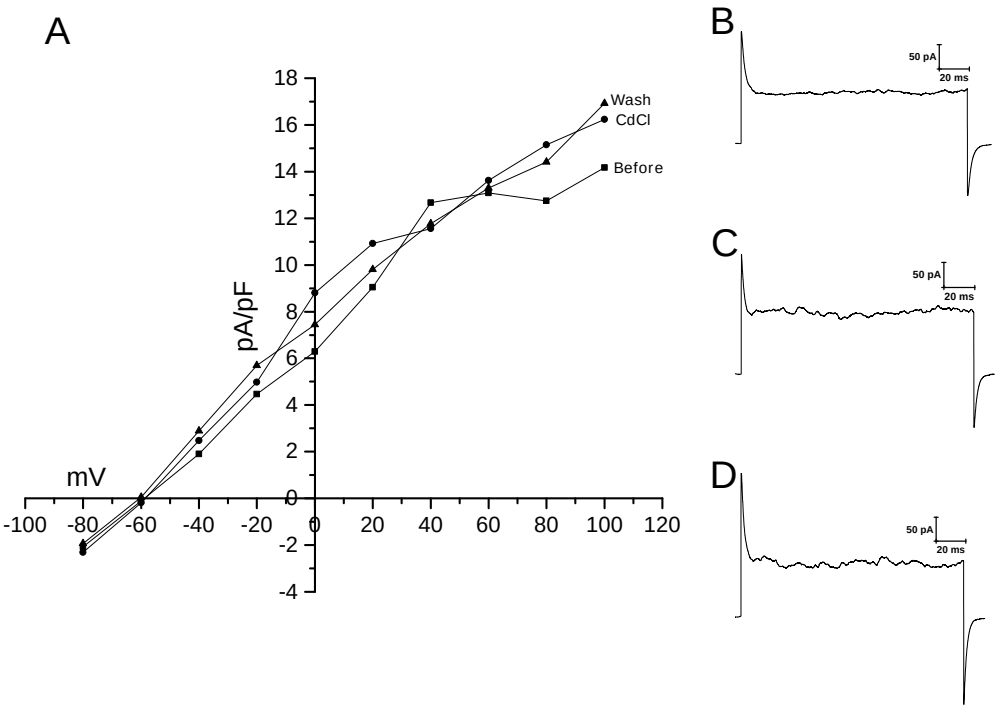

Figure 37. Calcium channel inhibitor on a NSPC treated with HASH1 + EGF for 2 weeks. The current-density (pA/pF) versus voltage (mV) plot at 50 ms for a NSPC grown with HASH1 + EGF in vitro for two weeks in ERS (before), CdCl, and a wash with ERS is shown (A). The current (pA) of the NSPC when held at 20 mV in ERS (B), CdCl (C), and wash with ERS (D).

Chapter 4. Discussion

The differentiation of neurons from various stem cell niches of the of the brain is of importance to understand the development of the nervous system better, as well as to direct the differentiation of stem cells in regenerative medicine. The main goals of this thesis were to drive NSPCs to neurons, and to determine whether these differentiated cells were functional. To test this functionality, I used electrophysiology. Furthermore, using an in-house biosensor system, I wanted to determine whether neurons released glutamate from functional axons.

4.1. Glutamate sensitive outside-out patch

The extrasynaptic release of glutamate from non-myelinated axons is hypothesized to serve as a differentiation cue for OPCs. Glutamate release from axons has been detected from whole cell recordings of OPCs within the corpus callosum (Kukley *et al.*, 2007). In order to identify whether cells are releasing glutamate from either the axonal process or the synaptic cleft, we have previously developed HEK293T cells expressing GRIK3. This approach is novel in that is has the potential to identify exact locations of neurotransmitter release. The increase in membrane potential in outside-out patches following addition of glutamate in a whole bath solution provides evidence that the biosensor was functional. During a current-clamp, after glutamate binds to the GRIK3 receptor, there would be an inward Na^+ current that would cause an increase in membrane potential, just as seen in my recordings. In other systems, detection of glutamate with a sniffer patch has been performed by creating excised patches of pyramidal neurons in the hippocampus (Maeda *et al.*, 1995); however, to my

knowledge, this is the first time that excised patches with GRIK3 have been created and used from HEK293T cells.

During outside-out patch recordings, a patch was found to contain an ion channel, most likely other than GRIK3. A glutamate current would only be observed in the presence of glutamate. However, this particular patch demonstrated a significant current in the absence of glutamate, as the membrane was stepped in various voltages. Given the concentrations of K^+ outside (5mM) and inside (135mM) the patch, with the Nernst equilibrium equation at room temperature, the equilibrium potential for K^+ would be -83 mV. The membrane potential of the outside-out patch was -73 mV, suggesting that the isolated membrane contained an ion channel that allowed for the movement of K^+. The difference in the calculated potential and the recorded potential may be due to slight inaccuracies in the K^+ concentrations in the recording solutions. This is unsurprising, given that K^+ channels are found on all cells, including the HEK293T and maintain resting membrane potentials (Kuang *et al.*, 2015).

In half of the whole cell trials, there was a response to glutamate; however, there were only three outside-out patches that responded to glutamate. The number of successful sniffer patches was relatively low compared to the cells that could theoretically respond to glutamate. For example, in HEK293T cells that had been programmed with a GABA receptor, the whole cell sniffer detected GABA in more than 80% of cells tested (Christensen *et al.*, 2014). Because a whole cell was being used, it was expected that the majority of the cells would have sufficient protein expression to be functional. In contrast, outside-out patches require that the ion channel of interest, or at least one channels, be isolated and that the patch conformation be correct. Therefore, it is

less likely to have receptors in the patch if the cells do not express the receptor at a high enough density.

The HEK293T cells expressing GRIK3 were produced via lentivirus transduction. The plasmid construct that allows for GRIK3 expression produces a GRIK3 fusion peptide with GFP and antibiotic resistance genes for selection. While the HEK293T cells did stain positive for GRIK3 and showed GFP expression, they may not have expressed the receptor at a high enough density. The probability of a channel opening with only a few receptors in the patch is low (Allen, 1997). This is likely the case with my results, because many of the donor cells responded to glutamate in the whole cell configuration, but the excised patches did not. Lentivirus can generate very stable HEK293T cell lines with prolonged expression of recombinant proteins (Mao *et al.*, 2015). Even with the capability of generating stable recombinant cell lines, expression of the protein can decrease over time. These HEK293T cells were only selected by antibiotics when they were produced; thus, this may allow for low expressers to have survived after this selection. Furthermore, with prolonged cell culture, the low expressers thrive because they express less GFP; expressing high levels of GFP is toxic to cells and puts them at a disadvantage compared to the low expressers (Ansari *et al.*, 2016). There are a few approaches, such as the addition of antibiotics, or keeping large stocks of frozen cells, to mitigate low expressers. Regular antibiotic selection with high concentrations to kill the low expresser would improve the responsiveness from the cells in the population.

Due to limitations in the experiment and difficulty of the technique, the extra-synaptic release of the neurotransmitter glutamate from DRG neurons was not tested.

While not advancing to the sniffer patch experiment of DRG neurons, I found that DRG neurons do have spontaneous activity because there were changes in the membrane potential at rest, suggesting that the DRGs can release neurotransmitter *in vitro*. In addition to sniffer patch experiments, the recordings from DRG neurons provided an electrophysiological profile to compare to differentiated cells. The large, negative current at higher potentials that was seen in the DRGs is from the inward flow of Na^+ into the cell through voltage-gated Na^+ channels.

4.2. Neural Differentiation with HASH1

ASH1 is a well-known transcription factor that induces neurogenesis. The addition of the cell permeable HASH1 fusion peptide to adult NSPCs *in vitro* caused changes in the electrophysiological profile and the expression of NF, indicating that the protein had an effect on the NSPCs. After two weeks of treatment, most of the cells did not develop into mature neurons capable of generating action potentials; therefore, they likely do not have enough voltage-gated Na^+ channels to generate an action potential. However, the HASH1 fusion peptide did have some effect on adult NSPCs and may promote differentiation. The withdrawal of the growth factor EGF was also tested in combination with HASH1 to determine the best condition for neurogenesis. The withdrawal of EGF from NSPCs caused increased expression of NF determined by immunocytochemistry. However, the electrophysiological profile remained the same as NSPCs cultured with EGF. In addition, there was no NF detected in neurites. Thus, the cells are not likely differentiating into neurons. The NSPCs were not immunostained for the astrocyte marker GFAP; as such, it cannot be ruled out that the NSPCs were becoming astrocytes. Typically, the withdrawal of EGF from NSPCs *in vitro* promotes

the majority of the cells to become $GFAP^+$ astrocytes (95%) and a small proportion to become neurons and OLs (Prüss *et al.*, 2011). It has, however, been reported that mitogen withdrawal induced 20-30% of cultured NSPCs to become neurons (Bonnert *et al.*, 2006). NSPCs treated with HASH1 ± EGF immunostained positive for NF and continued to proliferate at high rates similar to the control group, which suggests that the cells are becoming neurons, because ASH1 increases proliferation in NSPCs (Vasconcelos & Castro, 2014).

The expression profile of ion channels in NSPCs and neurons differ; therefore, the electrophysiological profile of the cell membrane can be used to determine not only the ion channel function, but also the cell type. The electrophysiological recordings showed that NSPCs treated with HASH1 had larger whole cell currents compared to NSPCs not treated with HASH1 after one week. In contrast, NSPCs treated with HASH + EGF had lower whole cell currents than the other treatment groups after two weeks. The currents recorded were whole cell currents; thus, they are a sum of the inward and outward currents. The higher currents recorded in NSPCs treated with HASH1 in week one would be a result of K^+ channel currents because the outward current is positive. NSPCs derived from the SVZ express many types of K^+ channels including two-pore, inward rectifying and voltage-gated K^+ channels (Prüss *et al.*, 2011). Therefore, the increase in current seen in the week one treatment may have been from an increase in K^+ channel expression in NSPCs treated with HASH1. The decrease of whole cell current in the HASH1 + EGF treated compared to the other groups, may be from the presence of voltage-gated Na^+ channels.

The presence of voltage-gated Na^+ channels indicates that the cells are likely functional neurons, due to the involvement of these ion channels in the generation of action potentials. NSPCs do not express voltage-gated Na^+ channels (Hogg *et al.*, 2004). The inward current observed following the capacitive transient in more than 50 % of the cells within all treatment groups, more frequently in the one week experiment, was unlikely from voltage-gated Na^+ channels because the addition TTX did not remove the inward current following the capacitive transient and there was no change in whole cell currents of NSPCs in EGF. The addition of TTX to cells with voltage-gated Na^+ channels should increase the whole cell currents and prevent any inward current because TTX blocks inward current from voltage-gated Na^+ channels (Chong & Ruben, 2008). After the addition of TTX to a NSPC treated for HASH1 + EGF for two weeks, there was an increase in whole cell current that was reversible upon washing. This suggests the cells treated with HASH1 + EGF may express voltage-gated Na^+ channels. In addition, there was a NSPC treated with HASH1 + EGF for one week that had a similar electrophysiological profile to a neuron with large inward current at higher potentials. The HASH1 - EGF treated NSPCs had similar whole cell currents to the ±EGF treated groups after two weeks suggesting they do not express voltage-gated Na^+ channels; however, this was not tested thus future experiments are required.

4.3. Conclusions and future directions

The range of detection of the biosensor was not tested in the patches isolated. The next experiment would be to provide a range of concentrations that can be detected by the sniffer patch and the lowest concentration of glutamate that can be detected, because physiological concentrations are much lower in the brain (1-30 μM) (Moussawi *et al.*,

2011) than the 10 mM tested. Outside-out patches from neurons in the hippocampus have been used to detect glutamate in hippocampal slices, where the patch could detect 3 µM to 10 mM glutamate (Maeda *et al.*, 1995), demonstrating that low concentrations can be detected. However, to detect low concentrations the patch needs to have a high density of receptors; it has been reported for acetylcholine detection from a sniffer patch a receptor concentration of 100 μm^{-1} was needed to detect 3 nM acetylcholine (as cited in Grinnell *et al.*, 1989).

After the sniffer patch is calibrated for glutamate detection, the next experiments would be co-culturing HEK293T with GRIK3 with DRG neurons and trying to detect glutamate release from axons. The co-culture experiments still require optimization prior to sniffing for glutamate. It was demonstrated that DRG neurons had small, spontaneous changes in membrane potential. While spontaneous activity was observed, it was not determined if DRG neurons could generate spontaneous action potentials and release glutamate. DRG neurons have been reported to release low basal levels of glutamate *in vitro* without stimulation (Rydh-Rinder *et al.*, 2001). Therefore, the neurons need to be stimulated to release detectable levels of glutamate. There are multiple approaches to evoke a neuron to release NTs; an additional electrode can be placed on the neuron or the K^+ concentration increased to depolarize the membrane (Allen, 1997). However, it has been demonstrated that high K^+ concentrations did not evoke the release of glutamate from DRG neurons *in vitro*; instead, the addition of bradykinin (BK), an inflammatory mediator, evoked the release of glutamate from DRG neurons (Rydh-Rinder *et al.*, 2001). BK induces the release of glutamate because DRG neurons are involved in nociception (pain) (Taguchi *et al.*, 2015) and inflammatory mediators activate DRG

neurons in nociception (Davidson *et al.*, 2014). Therefore, BK could be used in future experiments to promote glutamate release in culture.

This thesis shows that the addition of the HASH1 fusion peptide can induce electrophysiological changes in adult NSPCs and induce the expression of NF. The HASH1 fusion peptide likely has the potential to induce differentiation of adult NSPCs into neurons *in vitro*. The induction of neural differentiation with this HASH1 peptide has also been demonstrated with human iPSCs after 8 days (Robinson *et al.*, 2016). The shortened time for differentiation may be a result of the different cell types and regenerative capabilities. Differentiation by ASH1 is most commonly induced by transfecting cells to express the gene of interest. With this method, it has been reported that ASH1 alone can reprogram astrocytes to neurons (Ding *et al.*, 2014; Liu *et al.*, 2015).

Interestingly, the expected optimal condition would be HASH1 - EGF, but the electrophysiology data suggests that HASH1 + EGF was the optimal condition for differentiation because this was the only group with inward Na^+ currents. However, the HASH1 - EGF condition cannot be ruled out because the sample set was small and the immunocytochemistry shows increased NF. The conclusion of this study is that the cells need more time to develop into functional neurons, as the current profile was that of an immature neuron. It has been demonstrated in other *in vitro* systems that neural differentiation can take up to 18 days (Hogg *et al.*, 2004). *In vivo* differentiation can take 2-4 weeks (Winner *et al.*, 2002).

One limitation to growing cells for a longer period of time (3+ weeks) is the extensive cell proliferation observed. This led to high confluency in a short period of time, reducing the ability to perform either immunocytochemistry or electrophysiological analyses of the cells. It was difficult to seed the cells at a low density as they did not thrive. An approach to performing longer experiments and reducing confluency problems would be to culture the cells on a larger surface for the first week, then move the cells to coverslips for the following two weeks to allow for possible neurite growth. However, this added manipulation could result in modifications in gene expression and affect cell behavior by detaching the cells.

It is challenging to initiate neurogenesis in cell culture, as the *in vivo* environment provides different cues during neurogenesis. It has been reported that electrical inputs are required for neural development (Deisseroth *et al.*, 2004; Lledo & Saghatelyan, 2005). Furthermore, the *in vivo* environment is enriched with growth factors and neurotransmitters. Additional growth factors in combination with HASH1 may improve the generation of functional neurons from adult NSPCs. Another factor to consider in differentiating adult NSPCs is that regenerative capacity declines with age (Molofsky *et al.*, 2006). The mechanisms of age related decline of neurogenesis remains unclear. It has been suggested that NSPCs lose their ability to respond to differentiation cues (Ruckh *et al.*, 2012) or a decline of proliferation in the NSPCs (Molofsky *et al.*, 2006). Age related decline has also been observed in OPCs and decreased myelination (Franklin & Kotter, 2008).

The NSPCs from the SVZ are destined to become OB neurons; however, culturing NSPCs *in vitro* in the presence of EGF makes them multipotent, capable of

also generating glial cell lineages. Thus, culturing NSPCs for long periods of time with EGF may have a long-term effect on neurogenesis and reduce responsiveness to neural differentiation cues. Performing experiments at lower passages and minimal exposure to EGF would help mitigate this problem.

Due to the general bias in the electrophysiology data, flow cytometry would be useful to accompany this data because it is difficult to draw conclusions with a small sample set. Flow cytometry can give an indication of what proportion of cells are expressing neural and glial cell markers and the intermediate cell markers. Additional ion channel inhibitor experiments should be done to identify expression profile to provide more conclusive data and determine which ion channel is responsible for the inward and outward currents observed at higher potentials. There were only a few trials with voltage sodium and calcium inhibitors and no trials with voltage potassium channel inhibitors. Therefore it cannot be ruled out that the transient inward current was not from calcium channels because activation of Ca^{2+} channels produces negative, inward current and the reversal potential of calcium channels are at positive potentials. Furthermore, experiments with ion channel inhibitors (K^+, Na^+, Ca^{2+}) at different time points would help in determining if and when voltage-gated sodium channels develop, and if they are capable of generating action potentials.

Finally, neurons generated from adult NSPCs with expression of ASH1 can develop into glutamatergic neurons (Kim *et al.*, 2007); therefore, neurons generated from the addition of HASH1 *in vitro* may be capable of releasing glutamate. Once mature neurons can be developed, the glutamate sniffer patch could be used to try to detect extrasynaptic release of glutamate from neurons generated from HASH1.

References

Aiba, K., Sharov, A.A., Carter, M.G., Foroni, C., Vescovi, A.L., & Ko, M.S.H. (2006) Defining a developmental path to neural fate by global expression profiling of mouse embryonic stem cells and adult neural stem/progenitor cells. *Stem Cells*, **24**, 889-895.

Akaike, N. & Harata, N. (1994) Nystatin Perforated Patch Recording and Its Applications to Analyses of Intracellular Mechanisms. *Jpn. J. Physiol.*, **44**, 433-473.

Allen, T.G.J. (1997) The "sniffer-patch" technique for detection of neurotransmitter release. *Trends Neurosci*, **5**, 195-197.

Altman, J. & Das, G.D. (1965) Autoradiographic and histological evidence of postnatal hippocampal neurogenesis in rats. *J. Comp. Neurol.*, **124**, 319-335.

Ansari, A.M., Ahmed, A.K., Matsangos, A.E., Lay, F., Born, L.J., Marti, G., Harmon, J.W., & Sun, Z. (2016) Cellular GFP Toxicity and Immunogenicity: Potential Confounders in in Vivo Cell Tracking Experiments. *Stem Cell Rev. Reports*,.

Barateiro, A. & Fernandes, A. (2014) Temporal oligodendrocyte lineage progression: In vitro models of proliferation, differentiation and myelination. *Biochim. Biophys. Acta - Mol. Cell Res.*, **1843**, 1917-1929.

Bercury, K.K. & Macklin, W.B. (2015) Dynamics and mechanisms of CNS myelination. *Dev. Cell*, **32**, 447-458.

Bez, A., Corsini, E., Curti, D., Biggiogera, M., Colombo, A., Nicosia, R.F., Pagano, S.F., & Parati, E.A. (2003) Neurosphere and neurosphere-forming cells: Morphological and ultrastructural characterization. *Brain Res.*, **993**, 18-29.

Bonnert, T.P., Bilsland, J.G., Guest, P.C., Heavens, R., McLaren, D., Dale, C., Thakur, M., McAllister, G., & Munoz-Sanjuan, I. (2006) Molecular characterization of adult mouse subventricular zone progenitor cells during the onset of differentiation. *Eur.*

J. Neurosci., **24**, 661-675.

Castillo, P.E., Malenka, R.C., & Nicoll, R.A. (1997) Kainate receptors mediate a slow postsynaptic current in hippocampal CA3 neurons. *Nature*, **388**, 182-186.

Castro, D.S., Martynoga, B., Parras, C., Ramesh, V., Pacary, E., Johnston, C., Drechsel, D., Lebel-Potter, M., Garcia, L.G., Hunt, C., Dolle, D., Bithell, A., Ettwiller, L., Buckley, N., & Guillemot, F. (2011) A novel function of the proneural factor Ascl1 in progenitor proliferation identified by genome-wide characterization of its targets. *Genes Dev.*, **25**, 930-945.

Cavaliere, F., Urra, O., Alberdi, E., & Matute, C. (2012) Oligodendrocyte differentiation from adult multipotent stem cells is modulated by glutamate. *Cell Death Dis.*, **3,** 10.1038/cddis.2011.144.

Chanda, S., Ang, C.E., Davila, J., Pak, C., Mall, M., Lee, Q.Y., Ahlenius, H., Jung, S.W., Südhof, T.C., & Wernig, M. (2014) Generation of Induced Neuronal Cells by the Single Reprogramming Factor ASCL1. *Stem Cell Reports*, **3**, 282-296.

Chittajallu, R., Vignes, M., Dev, K.K., Barnes, J.M., Collingridge, G.L., & Henley, J.M. (1996) Regulation of glutamate release by presynaptic kainate receptors in the hippocampus. *Nature*, **379**, 78-81.

Chong, H.L. & Ruben, P.C. (2008) Interaction between voltage-gated sodium channels and the neurotoxin, tetrodotoxin. *Channels*, **2**, 407-412.

Christensen, R.K., Petersen, A. V, Schmitt, N., & Perrier, J.-F. (2014) Fast detection of extrasynaptic GABA with a whole-cell sniffer. *Front. Cell. Neurosci.*, **8**, 10.3389/fncel.2014.00133.

Curtis, D.R., Phillis, J.W., & Watkins, J.C. (1960) The chemical excitation of spinal neurones by certain acidic amino acids. *J. Physiol.*, **150**, 656-682.

D'Souza, B., Miyamoto, A., & Weinmaster, G. (2008) The many facets of Notch ligands. *Oncogene*, **27**, 5148-5167.

Davidson, S., Copits, B.A., Zhang, J., Page, G., Ghetti, A., & Gereau, R.W. (2014) Human sensory neurons: Membrane properties and sensitization by inflammatory mediators. *Pain*, **155**, 1861-1870.

Deisseroth, K., Singla, S., Toda, H., Monje, M., Palmer, T.D., & Malenka, R.C. (2004) Excitation-Neurogenesis Coupling in Adult Neural Stem/Progenitor Cells. *Neuron*, **42**, 535-552.

Ding, D., Xu, L., Xu, H., Li, X., Liang, Q., Zhao, Y., & Wang, Y. (2014) Mash1 efficiently reprograms rat astrocytes into neurons. *Neural Regen. Res.*, **9**, 25-32.

Doetsch, F. (2003) A niche for adult neural stem cells. *Curr. Opin. Genet. Dev.*, **13**, 543-550.

Doetsch, F., García-Verdugo, J.M., & Alvarez-Buylla, A. (1997) Cellular Composition and Three-Dimensional Organization of the Subventricular Germinal Zone in the Adult Mammalian Brain. *J. Neurosci.*, **17**, 5046-5061.

Doetsch, F., Petreanu, L., Caille, I., Garcia-Verdugo, J.M., & Alvarez-Buylla, A. (2002) EGF converts transit-amplifying neurogenic precursors in the adult brain into multipotent stem cells. *Neuron*, **36**, 1021-1034.

Dong, X.X., Wang, Y., & Qin, Z.H. (2009) Molecular mechanisms of excitotoxicity and their relevance to pathogenesis of neurodegenerative diseases. *Acta Pharmacol. Sin.*, **30**, 379-387.

Dupree, J.L., Girault, J.A., & Popko, B. (1999) Axo-glial interactions regulate the localization of axonal paranodal proteins. *J. Cell Biol.*, **147**, 1145-1152.

Esposito, M.S., Paitti, V., Laplagne, D., Morgenstern, N., Ferrari, C., Pitossi, F., & Schinder, A.F. (2005) Neuronal Differentiation in the Adult Hippocampus Recapitulates Embryonic Development. *J. Neurosci.*, **25**, 10074-10086.

Fannon, J., Tarmier, W., & Fulton, D. (2015) Neuronal Activity and AMPA-type glutamate receptor activation regulates the morphological development of

oligodendrocyte precursor cells. *Glia*, **63**, 1021-1035.

Franklin, R.J.M. & Kotter, M.R. (2008) The biology of CNS remyelination : The key to therapeutic advances. In *Journal of Neurology*. pp. 19-25.

Gautier, H.O.B., Evans, K.A., Volbracht, K., James, R., Sitnikov, S., Lundgaard, I., James, F., Lao-Peregrin, C., Reynolds, R., Franklin, R.J.M., & Káradóttir, R.T. (2015) Neuronal activity regulates remyelination via glutamate signalling to oligodendrocyte progenitors. *Nat. Commun.*, **6**, 8518.

Ginhoux, F., Greter, M., Leboeuf, M., Nandi, S., See, P., Mehler, M.F., Conway, S.J., Ng, L.G., Stanley, E.R., Igor, M., & Merad, M. (2010) Fate mapping analysis reveals that adult microglia derive from primitive macrophages. *Science (80-.).*, **330**, 841-845.

Ginhoux, F., Lim, S., Hoeffel, G., Low, D., & Huber, T. (2013) Origin and differentiation of microglia. *Front. Cell. Neurosci.*, **7**, 45.

Grinnell, A.D., Gundersen, C.B., Meriney, S.D., & Young, S.H. (1989) Direct measurement of ACh release from exposed frog nerve terminals: constraints on interpretation of non-quantal release. *J. Physiol.*, **419**, 225-251.

Henke, R.M., Meredith, D.M., Borromeo, M.D., Savage, T.K., & Johnson, J.E. (2009) Ascl1 and Neurog2 form novel complexes and regulate Delta-like3 (Dll3) expression in the neural tube. *Dev. Biol.*, **328**, 529-540.

Hogg, R.C., Chipperfield, H., & Whyte, K.A. (2004) Functional maturation of isolated neural progenitor cells from the adult rat hippocampus. *Eur. J.*, **19**, 2410-2420.

Imayoshi, I. & Kageyama, R. (2014) bHLH factors in self-renewal, multipotency, and fate choice of neural progenitor cells. *Neuron*, **82**, 9-23.

Imayoshi, I., Sakamoto, M., Yamaguchi, M., Mori, K., & Kageyama, R. (2010) Essential Roles of Notch Signaling in Maintenance of Neural Stem Cells in Developing and Adult Brains. *J. Neurosci.*, **30**, 3489-3498.

Ishibashi, T., Dakin, K.A., Stevens, B., Lee, P.R., Kozlov, S. V, Stewart, C.L., & Fields, R.D. (2006) Astrocytes promote myelination in response to electrical impulses. *Neuron*, **49**, 823-832.

Johe, K.K., Hazel, T., Muller, T., Dugich-Djordjevic, & Mckay, R. (1996) Single factors direct the differentiation of stem cells from the fetal and adult central nervous system. *Genes Dev.*, **10**, 3129-3140.

Kaplan, M.S. & Bell, D.H. (1984) Mitotic neuroblasts in the 9-day-old and 11-month-old rodent hippocampus. *J. Neurosci.*, **4**, 1429-1441.

Khakh, B.S. & Sofroniew, M. V (2015) Diversity of astrocyte functions and phenotypes in neural circuits. *Nat. Neurosci.*, **18**, 942-952.

Kim, E.J., Leung, C.T., Reed, R.R., & Johnson, J.E. (2007) In Vivo Analysis of Ascl1 Defined Progenitors Reveals Distinct Developmental Dynamics during Adult Neurogenesis and Gliogenesis. *J. Neurosci.*, **27**, 12764-12774.

Kleckner, N.W. & Dingledine, R. (1988) Requirement for Glycine in Activation of NMDA-Receptors Expressed in Xenopus Oocytes. *Science (80-.).*, **241**, 835-837.

Krames, E.S. (2014) The role of the dorsal root ganglion in the development of neuropathic pain. *Pain Med. (United States)*, **15**, 1669-1685.

Kuang, Q., Purhonen, P., & Hebert, H. (2015) Structure of potassium channels. *Cell. Mol. Life Sci.*, **72**, 3677-3693.

Kukley, M., Capetillo-Zaratche, E., & Deitrich, D. (2007) Vesicular glutamate release from axons in white matter. *Nat. Neurosci.*, **10**, 311-320.

Lerma, J. (2003) Roles and rules of kainate receptors in synaptic transmission. *Nat. Rev. Neurosci.*, **4**, 481-495.

Li, C., Xiao, L., Liu, X., Yang, W., Shen, W., Hu, C., Yang, G., & He, C. (2013) A functional role of NMDA receptor in regulating the differentiation of

oligodendrocyte precursor cells and remyelination. *Glia*, **61**, 732-749.

Liu, R., Lin, G., & Xu, H. (2013) An efficient method for dorsal root ganglia neurons purification with a one-time anti-mitotic reagent treatment. *PLoS One*, **8**, e60558.

Liu, Y., Miao, Q., Yuan, J., Han, S., Zhang, P., Li, S., Rao, Z., Zhao, W., Ye, Q., Geng, J., Zhang, X., & Cheng, L. (2015) Ascl1 Converts Dorsal Midbrain Astrocytes into Functional Neurons In Vivo. *J. Neurosci.*, **35**, 9336-9355.

Lledo, P.M. & Saghatelyan, A. (2005) Integrating new neurons into the adult olfactory bulb: Joining the network, life-death decisions, and the effects of sensory experience. *Trends Neurosci.*, **28**, 248-254.

Lois, C. & Alvarez-Buylla, A. (1993) Proliferating subventricular zone cells in the adult mammalian forebrain can differentiate into neurons and glia. *Proc. Natl. Acad. Sci.*, **90**, 2074-2077.

Lois, C., Garcia-Verdugo, J.M., & Alvarez-Buylla, A. (1996) Chain migration of neuronal precursors. *Science*, **271**, 978-981.

Lüscher, C. & Malenka, R.C. (2012) NMDA receptor-dependent long-term potentiation and long-term depression (LTP/LTD). *Cold Spring Harb. Perspect. Biol.*, **4**, 1-15.

Maeda, T., Shimoshige, S., Mizukami, K., Shimohama, S., Kaneko, S., Kaike, A., & Satoh, M. (1995) Patch sensor detection of glutamate release evoked by a single electrical shock. *Neurotechnique*, **15**, 253-257.

Mao, Y., Yan, R., Li, A., Zhang, Y., Li, J., Du, H., Chen, B., Wei, W., Zhang, Y., Sumners, C., Zheng, H., & Li, H. (2015) Lentiviral vectors mediate long-term and high efficiency transgene expression in HEK 293T cells. *Int. J. Med. Sci.*, **12**, 407-415.

Matsuzaki, M., Honkura, N., Ellis-Davies, G.C.R., & Kasai, H. (2004) Structural basis of long-term potentiation in single dendritic spines. *Nature*, **429**, 761-766.

Molofsky, A. V., Slutsky, S.G., Joseph, N.M., He, S., Pardal, R., Krishnamurthy, J., Sharpless, N.E., & Morrison, S.J. (2006) Increasing p16INK4aexpression decreases forebrain progenitors and neurogenesis during ageing. *Nature*, **443**, 448-452.

Morrison, B.M., Lee, Y., & Rothstein, J.D. (2013) Oligodendroglia: metabolic supporters of axons. *Trends Cell Biol.*, **23**, 644-651.

Moussawi, K., Riegel, A., Nair, S., & Kalivas, P.W. (2011) Extracellular Glutamate: Functional Compartments Operate in Different Concentration Ranges. *Front. Syst. Neurosci.*, **5**, 1-9.

Nakatani, H., Martin, E., Hassani, H., Clavairoly, A., Maire, C.L., Viadieu, A., Kerninon, C., Delmasure, A., Frah, M., Weber, M., Nakafuku, M., Zalc, B., Thomas, J.-L., Guillemot, F., Nait-Oumesmar, B., & Parras, C. (2013) Ascl1/Mash1 promotes brain oligodendrogenesis during myelination and remyelination. *J. Neurosci.*, **33**, 9752-9768.

Neher, E. (1992) Nobel lecture. ion channels for communication between and within cells. [review]. *Neuron*, **8**, 605-612.

Neher, E. & Sakmann, B. (1976) Single-channel currents recorded from membrane of denervated frog muscle fibres. *Nature*, **260**, 799-802.

Penner, R. (2009) A Practical Guide to Patch Clamping. In *Single-Channel Recording*. pp. 3-28.

Pierre-Marie, L., Merkle, F.T., & Alvarez-Buylla, A. (2014) Origin and function of olfactory bulb interneuron diversity. *Trends Neurosci.*, **31**, 392-400.

Ponti, G., Obernier, K., Guinto, C., Jose, L., Bonfanti, L., & Alvarez-Buylla, A. (2013) Cell cycle and lineage progression of neural progenitors in the ventricular-subventricular zones of adult mice. *Proc. Natl. Acad. Sci. U. S. A.*, **110**, E1045-54.

Prüss, H., Dewes, M., Derst, C., Fernández-Klett, F., Veh, R.W., & Priller, J. (2011) Potassium channel expression in adult murine neural progenitor cells.

Neuroscience, **180**, 19-29.

Reynolds, B. a & Weiss, S. (1992) Generation of neurons and astrocytes from isolated cells of the adult mammalian central nervous system. *Science*, **255**, 1707-1710.

Robinson, M., Chapani, P., Styan, T., Vaidyanathan, R., & Willerth, S.M. (2016) Functionalizing Ascl1 with Novel Intracellular Protein Delivery Technology for Promoting Neuronal Differentiation of Human Induced Pluripotent Stem Cells. *Stem Cell Rev. Reports*, **12**, 476-483.

Rosenmund, C., Stern-bach, Y., & Stevens, C.F. (1997) The Tetrameric Structure of a Glutamate Receptor Channel. *Science (80-.).*, **280**, 1596-1599.

Ruckh, J.M., Zhao, J.-W., Shadrach, J.L., van Wijngaarden, P., Rao, T.N., Wagers, A.J., & Franklin, R.J.M. (2012) Rejuvenation of Regeneration in the Aging Central Nervous System, Cell Stem Cell.

Rydh-Rinder, M., Kerekes, N., Svensson, M., & Hökfelt, T. (2001) Glutamate release from adult primary sensory neurons in culture is modulated by growth factors. *Regul. Pept.*, **102**, 69-79.

Sakmann, B. & Neher, E. (1984) Patch clamp techniques for studying ionic channels in excitable membranes. *Annu. Rev. Physiol.*, **46**, 455-472.

Seri, B., Garcia-Verdugo, J.M., McEwen, B.S., & Alvarez-Buylla, A. (2001) Astrocytes give rise to new neurons in the adult mammalian hippocampus. *J. Neurosci.*, **21**, 7153-7160.

Shaw, E. & Compston, S. (1996) Analysis of lntegrin Interaction Expression on Oligodendrocytes during by Using Rat-Mouse Xenocultures. *J. Cell Sci.*, **76**, 1163-1172.

Sobolevsky, A.I., Rosconi, M.P., & Gouaux, E. (2009) X-ray structure, symmetry and mechanism of an AMPA-subtype glutamate receptor. *Nature*, **462**, 745-756.

Stevens, B., Porta, S., Haak, L.L., Gallo, V., & Fields, R.D. (2002) Adenosine: A neuron-glial transmitter promoting myelination in the CNS in response to action potentials. *Neuron*, **36**, 855-868.

Taguchi, T., Katanosaka, K., Yasui, M., Hayashi, K., Yamashita, M., Wakatsuki, K., Kiyama, H., Yamanaka, A., & Mizumura, K. (2015) Peripheral and spinal mechanisms of nociception in a rat reserpine-induced pain model. *Pain*, **156**, 415-427.

Traynelis, S.F., Wooollmuth, L.P., McBAin, C.J., Menniti, F.S., Vance, K.N., Ogden, K.K., Hansen, K.B., Yuan, H., Myers, S.J., & Dingledine, R. (2010) Glutamate receptor ion channels: structure, regulation and function. *Pharmacol. Rev.*, **62**, 405-496.

van Praag, H., Schinder, A.F., Christie, B.R., Toni, N., Palmer, T.D., & Gage, F.H. (2002) Functional neurogenesis in the adult hippocampus. *Nature*, **415**, 1030-1034.

Vasconcelos, F.F. & Castro, D.S. (2014) Transcriptional control of vertebrate neurogenesis by the proneural factor Ascl1. *Front. Cell. Neurosci.*, **8**, 412.

Willard, S.S. & Koochekpour, S. (2013) Glutamate, glutamate receptors, and downstream signaling pathways. *Int. J. Biol. Sci.*, **9**, 948-959.

Winner, B., Cooper-Kuhn, C.M., Aigner, R., Winkler, J., & Kuhn, H.G. (2002) Long-term survival and cell death of newly generated neurons in the adult rat olfactory bulb. *Eur. J. Neurosci.*, **16**, 1681-1689.

Yeung, M.S.Y., Zdunek, S., Bergmann, O., Bernard, S., Salehpour, M., Alkass, K., Perl, S., Tisdale, J., Possnert, G., Brundin, L., Druid, H., & Fris??n, J. (2014) Dynamics of oligodendrocyte generation and myelination in the human brain. *Cell*, **159**, 766-774.

Young, K.M., Psachoulia, K., Tripathi, R.B., Dunn, S.J., Cossell, L., Attwell, D., Tohyama, K., & Richardson, W.D. (2013) Oligodendrocyte dynamics in the healthy adult CNS: Evidence for myelin remodeling. *Neuron*, **77**, 873-885.

Zhang, Y., Pak, C., Han, Y., Ahlenius, H., Zhang, Z., Marro, S., Patzke, C., Acuna, C., Covy, J., Yang, N., Danko, T., Chen, L., Wernig, M., Thomas, C., & Drive, C. (2013) Rapid Sngle-Step Induction of Functional Neurons from Human Pluripotent Stem Cells. *Neuron*, **78**, 785-798.

Zhao, C., Deng, W., & Gage, F.H. (2008) Mechanisms and functional implications of adult neurogenesis. *Cell*, **132**, 645-660.